2. SEISMIC REFLECTION STRATIGRAPHY OF LEG 184, SOUTH CHINA SEA[1]

Shipboard Scientific Party[2]

INTRODUCTION

The continental margins of the South China Sea (SCS) reflect a complex structural history of deposition related to rifting and subsidence as well as to climate and sea level–related depositional processes. Briefly, the original rifting of the SCS is thought to have begun in the Paleogene and continued until the Oligocene (~32 Ma). The continental crust of the northern continental margin was initially faulted, and then the margin subsided to develop a series of down-dropped blocks that filled with syn-rift sediments. Following the initial rifting and subsidence, active seafloor spreading began in the mid-Oligocene (~32 Ma) and continued until the middle Miocene (~16–17 Ma) (Taylor and Hayes, 1983; Briais et al., 1993). During both rifting and spreading phases, the outer subsiding margin was draped with terrigenous and hemipelagic sediments that were deposited and modified by mass wasting and current-related processes. Several magmatic intrusion events have added to the complexity of the margin. The margin is now characterized by an irregular series of sediment-filled basins and ridges. Several of the sites located in the northern SCS lie in the midslope basins (Sites 1144 and 1146) and on the subsided blocks (Sites 1145 and 1147/1148). In the southern SCS, part of the margin is characterized by a series of blocks, islands, and banks that are relatively uncharted and referred to as the Dangerous Grounds or Nansha Islands area. These features are thought to be underlain by a rifted continental crust that developed carbonate platforms and banks during the Neogene. Site 1143 lies among these features.

Much of the sediment deposition in the South China Sea is related to mass wasting processes (i.e., slumping, debris flows, and turbidites) (Damuth, 1979, 1980a; Wu et al., 1999). Maps of the 3.5-kHz echo char-

acteristics show that Sites 1144–1148 lie within the type IIIB characteristic, which is indicative of mass slumping and downslope transport (Damuth, 1980b). Others (Sarnthein et al., 1994) have suggested that thermohaline contour currents may produce similar echo characteristics and morphology in the SCS.

Given the complex geologic history of the South China Sea, both the selection of coring sites and the interpretation of their regional context and depositional history require establishing the seismic stratigraphy of the sites. The initial selection of Site 1143 was based on the Guangzhou Marine Geological Survey (GMGS), Ministry of Land and Resources of China, and Nansha Survey multichannel lines (NS and NSL) in the southern SCS. Sites 1144–1148 (SCS-1, -2, -4, and -5C) were originally chosen using SONNE95 seismic data (Lines 5, 10, and 20). Unfortunately, cross tracks for Sites 1145, 1146 and 1148 did not exist in the seismic data bank. Therefore, the Pollution Prevention and Safety Panel (PPSP) required Leg 184 scientists to acquire crossing seismic lines as part of the final site approval. The *JOIDES Resolution* scientific party carried out a single-channel seismic survey of proposed sites SCS-4 (1146), -5C (1148), and alternate -5E (contingency site; not drilled) on 12–13 March 1999. The seismic data were processed aboard the *JOIDES Resolution,* and critical sections were faxed to the Ocean Drilling Program, Texas A&M University, for final approval of the sites and penetration depths. A summary of all seismic lines and sections used to select and evaluate Leg 184 sites is given in Table **T1.**

In this chapter, we summarize the characteristics of various seismic reflection systems used to collect the data, review seismic reflection and 3.5-kHz records of each site, and relate seismic stratigraphy to the drilling results through the use of acoustic impedance logs.

SEISMIC SYSTEMS AND DATA

JOIDES Resolution

Leg 184 used the standard *JOIDES Resolution* configuration of single-channel seismic reflection equipment, as modified from the description of Comas, Zahn, Klaus, et al. (1996). The survey was conducted using an 80-in^3 water gun, which was towed ~20 m behind the stern at a depth of ~13 m to prevent it from broaching during the swell conditions. The gun was fired at 10-s intervals with ~2000 psi. The ship's speed was ~5 to ~6 kt depending on conditions. The hydrophone streamer was a 100-m Teledyne model 178, which contains 60 active hydrophones. The streamer was towed at a depth of ~15–20 m. The midpoint of the active portion of the streamer lay ~250 m astern. Analog seismic reflection data were displayed on Raytheon model 1807M and EPC model 9802 recorders. The seismic signal was digitized in real time and displayed on a Sun workstation and for processing. The data were written to DAT (4 mm) and Exabyte (8 mm) tapes in SEGY format. Shipboard processing used the SIOSEIS software and included automatic gain control and filtering to sharpen the signal.

The 3.5-kHz seismic system aboard the *JOIDES Resolution* consists of an EDO 248C transceiver mounted in a sonar dome and a Raytheon model 1807M line scanner recorder. The system has an effective acoustic cone of ~20° to ~30°. Only analog 3.5-kHz records are available for the Leg 184 site locations.

SONNE95

SONNE95, Legs 1 and 2 (April–May 1994), collected 2972 km of seismic reflection profiles on the northern continental margin of the South China Sea, mostly near the Pearl River Mouth Basin (Sarnthein et al., 1994). The seismic reflection system consisted of four air guns (three Geco Prakla and one SSI) with a total volume of 8.7 L. The guns were triggered at 25-m intervals, which at 4.5 kt gives a seismic record every 11 s. The signal was received by a Geco Prakla eight-channel hydrophone streamer, which had receiver-to-receiver distance of 12.5 m and a common midpoint distance of 6.25 m. Processing of the digital data was accomplished using the SEISTRIX 3 software and included digital filtering, muting, trace editing normal move-out correction, stacking, deconvolution, and migration (Wong et al., 1994).

SONNE95 used the PARASOUND profiling system, which has a narrow beam (~4°) that uses a differential frequency of ~4 kHz. This system increases vertical resolution and suppresses hyperbolic echoes where the surface slopes are low. Only analog PARASOUND records are available for the Leg 184 site locations.

Acoustical Impedance

Comparisons between the reflector sequences observed in the seismic lines and the characteristics of the sediment cores and logs were made by calculating the acoustical impedance as a function of two-way traveltime (TWT). Acoustical impedance was estimated as the product of the sonic velocity (meters per second) from the long-spaced sonic log and the hostile environment lithodensity sonde bulk density (g/cm^3) from the logged section of each site. The acoustical impedance was then smoothed with a 30-point moving window (~15 m in length) to eliminate the spikes caused by poor hole conditions but preserve the major impedance features. To calculate the TWT for each impedance estimate, we first smoothed the velocity data with a 30-m (67 points) moving window to approximate the seismic wavelength and give a smooth velocity structure for calculating depth relationships. We next calculated the interval TWT between logging measurements (TWT = $[2 \cdot D]/V$, where D = depth interval between log measurements in meters and V = smoothed velocity). These interval TWTs were cumulatively summed up from an initial depth, which varies from site to site depending on the hole conditions and on where the logs became reliable. We used the physical properties core-log data for bulk density and P-wave velocity to span the gap from core top to the logged interval. These shipboard values are usually lower than the in situ log values and have been adjusted to best fit the log data and give a continuous density and velocity profile for each site (see "Site 1143 [SCS-9]," p. 4; "Site 1144 [SCS-1]," p. 5; "Site 1145 [SCS-2]," p. 6; "Site 1146 [SCS-4]," p. 7; and "Sites 1147 and 1148 [SCS-5C]," p. 8). Because the reflection of seismic waves is sensitive to the relative change in impedance as well as the absolute amplitude, we examined the first derivative of the acoustical impedance log for some sites. These data will be presented in the Leg 184 *Scientific Results* volume of the *Proceedings of the Ocean Drilling Program*.

Seismic Reflector Stratigraphy

As noted by Ludmann and Wong (1999), "The nomenclature of sequences and unconformities in the Pearl River Mouth Basin is not unambiguous in the literature." This comment applies to the remainder of the SCS as well because several systems of seismic reflector (and associated or assumed unconformities and sequence boundaries) use the same symbols but assign different ages to the features. We follow the nomenclature of Ludmann and Wong (1999), who modified the system of Guong et al. (1989) for both sequences and unconformities. However, we include Pliocene/Pleistocene Reflector T_N from Jiang et al. (1994; see Fig. F6, p. 50, in the "Leg 184 Summary" chapter) and the Oligocene/Miocene Reflector T_5 from Chen et al. (1987; as illustrated in table 1 of Ludmann and Wong, 1999). The nomenclature and age assignments for these boundaries and their associated reflectors are summarized in Table T2.

Briefly, we adopt T_0 as a late Pleistocene reflector at ~0.45 Ma and T_N as the Pliocene/Pleistocene reflector at ~1.85 Ma. T_1 is taken as the Miocene/Pliocene reflector (~5.2 Ma), T_2 is the middle/upper Miocene reflector at ~10.2 Ma, and T_4 marks the lower/middle Miocene boundary at ~14–15 Ma. Although Ludmann and Wong (1999) do not recognize T_5 (Chen et al., 1987; ~26 Ma) in the Pearl River Mouth Basin, we retain it: some of the Leg 184 reflectors seem consistent with this age feature. Ludmann and Wong (1999) consider T_7 (~32 Ma) to be the mid-Oligocene breakup unconformity associated with the Nanhui Movement. This boundary marks the end of the rifting and the beginning of the drifting phase for the SCS basin. Although these reflectors are not always uniquely identified in the Leg 184 seismic lines and cores, they provide a useful frame of reference. The well-dated Leg 184 sediments may serve to better constrain the age of these features.

SEISMIC STRATIGRAPHY OF LEG 184 SOUTH CHINA SEA SITES

Site 1143 (SCS-9)

Site 1143 is located at 9°21.72′N, 113°17.10′E, at a water depth of 2772 m (Fig. F2, p. 46, in the "Leg 184 Summary" chapter; Fig. F1). Seismic data provided by the Guangzhou Marine Geological Survey was used to locate Site 1143 near the intersection of Lines NSL95-160 at CDP 1812 and NS95-240 at CDP 3617 (Figs. F1, F2). The basement structure and sediment cover near Site 1143 are complex with basement faulting on a scale of a few kilometers, and sediment thicknesses range from 700 to 1400 m (Fig. F2). A series of seismic reflectors, mapped by the GMGS, indicated that the proposed penetration of Site 1143 (400 meters below seafloor [mbsf]) should reach midway between Reflectors T_1 (top of the Miocene) and T_2 (top of the middle Miocene). Site 1143 is located in a slight depression within a fault basin that contains ~1.25 s (~1250 m) of sediment.

The *JOIDES Resolution* 3.5-kHz profiles on the approach to Site 1143 were highly parabolic, indicating an irregular surface on a scale of tens to hundreds of meters (Fig. F3). The 3.5-kHz profiles show that the site lies near the base of a slope in hummocky terrane that has a slightly diffuse echo character and sub-bottom reflectors at ~40 and 80 mbsf (Fig.

T2. Depth and age of reflectors, Leg 184, **p. 37.**

F1. Site 1143 located by precruise seismic survey lines, **p. 11.**
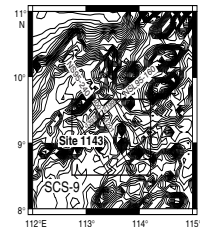
F2. Precruise seismic lines across Site 1143, **p. 12.**
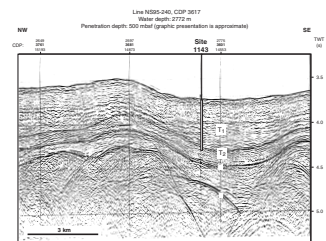
F3. 3.5-kHz record across Site 1143, **p. 14.**
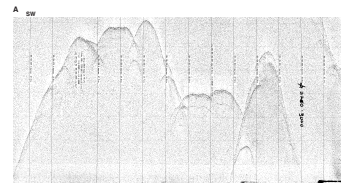
F3B). These echo characteristics are indicative of downslope transport (Damuth, 1980a, 1980b).

Seismic and Sediment Stratigraphy

The GMGS seismic reflection lines reveal major reflectors at ~0.27, ~0.55, ~0.67, and ~0.95 s TWT. The equivalent depths and ages for the upper two reflectors are ~210 (~5.2 Ma) and ~460 mbsf (~9.1 Ma) (Figs. F2, F4; Table T2). Hence, the upper reflector is consistent with T_1, but the second reflector at 0.55 TWT is somewhat younger than T_2. The impedance variations for the logged section (137 to 375 mbsf) of Hole 1143A show a rapid increase in impedance culminating ~0.27 s TWT or ~210–220 mbsf. The variability of impedance also decreases over this same interval. Following a brief reversal centered on ~260 mbsf, the impedance increases to ~340 mbsf (Fig. F4). The T_1 reflector appears to be coincident with the rapid increase in acoustical impedance between 200 and 240 mbsf. Although the logged section does not reach the next major reflector at 0.55 s, downward continuation of velocity data indicates that it lies at ~460 mbsf and was presumably penetrated in Hole 1143C, which was cored to 500 mbsf. Although the multisensor track and moisture and density measurements reach their maximum values between 400 and 500 mbsf, other properties do not give any indication of a shift that might cause the impedance peak. Downward continuation of velocity and age structure estimates that the reflector at 0.67 TWT lies at ~560 mbsf (~11.3 Ma) and the strong basal reflector at 0.95 TWT lies at ~820 mbsf (~17 Ma). Hence, the reflectors at 0.55 and 0.67 s seem to span the age (10.2 Ma) of the middle/upper Miocene Reflector T_2. These levels do fall within a sequence of rapidly accumulating and somewhat reworked sediments so that they may record local depositional processes associated with rapid filling of the basin.

In summary, the reflector sequence at Site 1143 does not conform well to the sequence derived from the northern SCS. Although the reflector at 0.27 roughly fits the T_1 age, the younger and older reflectors are not clearly identified at the drill site.

Site 1144 (SCS-1)

Site 1144 (SCS-1) is located at 20°03.18´N, 117°25.14´E, at a water depth of ~2037 m, which lies slightly above the sill depth of the Bashi Strait (2600 m) (see Fig. F9, p. 53, in the "Leg 184 Summary" chapter). The site is located on a thick sediment drift at the intersection of seismic Lines SONNE95-20 (CDP 3482) and SONNE95-10 (CDP 9600) (Figs. F5, F6). The drift nature of the site is indicated by its morphology and internal structure as well as by its high sedimentation rates. The sediment thickness above a prominent basinward dipping reflector is between ~0.75 and ~0.80 s, or ~610 to ~650 mbsf (Fig. F6). The seismic structure of the sediments is characterized by an upper reflector series (0–0.5 s) that has distinct, closely spaced reflectors and a lower, more diffuse zone (0.5–0.7 s) with less distinct reflectors. These diffuse seismic zones are often characteristic of slump or debris flow sediments (Damuth, 1980a, 1980b). The northwest-southeast dip line (SONNE95-10) reveals a wedge of sediment ranging from ~1725 to ~2400 m water depth. Internal reflectors indicate that the beds thin and pinch out in deeper water. The cross line (SONNE95-20) shows wavy reflectors, indicating possible drift or dunelike transport and redeposition of bottom sediments. Site 1144 is located near the center of the deposit, where

F4. Acoustical impedance record compared with seismic reflector stratigraphy, Site 1143, p. 16.
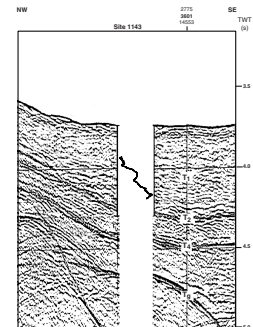
F5. Sites 1144–1148 located by precruise seismic survey lines, p. 17.
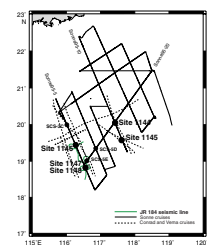
F6. Precruise seismic lines across Site 1144, p. 18.
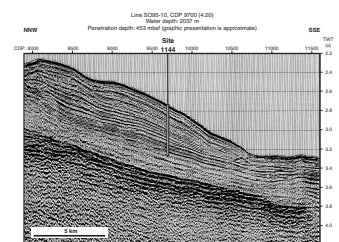
reflectors are relatively uniform and evenly structured on both lines. Given the sedimentation rates at this location, the base of Site 1144 (450 mbsf) lies well above the expected depth of the Pliocene/Pleistocene Reflector T_N).

The *JOIDES Resolution* 3.5-kHz and PARASOUND (Sarnthein et al., 1994) profiles across and on the approach to Site 1144 show thick sediments heavily draped over relief that locally is tens to hundreds of meters (Fig. F7). The well-defined, conformable sub-bottom reflectors indicate uniform sediment accumulation with systematic variations in sediment characteristics.

Seismic and Sediment Stratigraphy

A summary of the depth/age relations for Site 1144 reflectors is given in Table T2. At Site 1144, acoustical impedance was calculated from Hole 1144A over the interval 90–450 mbsf (see "Wireline Logging," p. 22, in the "Site 1144" chapter). The resulting plot of smoothed acoustical impedance as a function of TWT for Site 1144 is shown in Figure F8 along with the SONNE95-10 seismic section. Although the match is far from unique, several of the reflectors at Site 1144 coincide with rapid increases or decreases of acoustical impedance. The major reflector at ~0.47 s TWT (~370 mbsf) that divides the upper reflector zone from the more diffuse zone correlates with the major increase in acoustical impedance associated with increases in both velocity and density and is generally coincident with the boundary between lithologic Subunits 1C and 1B. This reflector also marks the top of the interval with high magnetic susceptibility (see "Physical Properties," p. 19, in the "Site 1144" chapter). The diffuse seismic zone is characterized by high density, high magnetic susceptibility, and a distinctly older age than the above reflector sequence. The age of this reflector is ~0.7 Ma and may reveal a hiatus or discontinuity in the section. Overall, the reflector sequence at Site 1144 displays the local depositional history within the Pleistocene.

Site 1145 (SCS-2)

Site 1145 is located at 19°35.04′N, 117°37.86′E, at a water depth of 3175 m. The site is at shotpoint 4704 on the seismic Line SONNE95-10 (Figs. F5, F9) on the lower of a series of terraces that form the continental slope off southern China. The northwest-southeast dip line (SO95-10) reveals sediments that are generally smooth and slightly onlapping onto the continental slope from the adjacent deep basin. The thick, conformable sediments extend almost 1 s below the seafloor (sbsf) to a strong wavy reflector, presumed to be basement (Fig. F9). Using the interval velocities provided by the Department of Marine Geology and Geophysics, Tongji University, this two-way traveltime is equivalent to ~760 m of sediment cover. The 200-mbsf penetration at Site 1145 reached only 0.28 sbsf. The seismic structure within the upper 200 mbsf contains an upper zone of multiple (about six) strong reflectors (0–0.12 sbsf) and a lower, more diffuse zone (0.12–0.28 sbsf) that is divided by a prominent reflector at ~0.21 sbsf (Fig. F9). A summary of the depth/age relations for Site 1145 reflectors is given in Table T2. The *JOIDES Resolution* 3.5-kHz data (Fig. F10) and SONNE95 PARASOUND data (Sarnthein et al., 1994) reveal relatively smooth, parallel conformable sediment cover with no distinct surface features.

F7. 3.5-kHz records at Site 1144, p. 20.
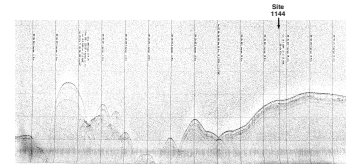
F8. Acoustical impedance record compared with seismic reflector stratigraphy, Site 1144, p. 21.
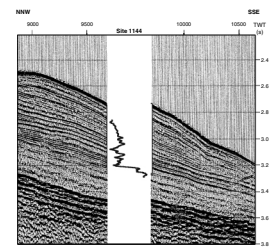
F9. Precruise seismic line across Site 1145, p. 22.
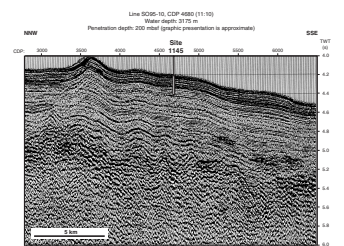
F10. 3.5-kHz records at Site 1145, p. 23.
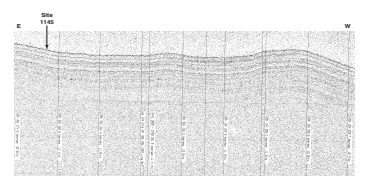
Seismic and Sediment Stratigraphy

Site 1145 was not wireline logged, so we do not have in situ *P*-wave velocity and density data. We used the velocity and density data from core measurements and the age model for Site 1145 to estimate the depth and age of the reflectors. The base of the surface reflector zone (0.12 s TWT) is estimated to be at a depth of ~85 mbsf with an age of ~0.6 Ma. The strong reflector at 0.21 s TWT is judged to be at ~160 mbsf with an age of ~1.87 Ma. Hence, this reflector is consistent with the age of the regional T_N reflector.

Site 1146 (SCS-4)

Site 1146 is located at 19°27.40′N, 116°16.37′E, at a water depth of 2092 m (see Fig. F9, p. 53, in the "Leg 184 Summary" chapter). The site was initially located on seismic Line SONNE95-5 at CDP 1049 within the thick sediment fill of a down-dropped block (Fig. F12). The *JOIDES Resolution* minisurvey obtained two crossing lines of the proposed Site SCS-4 to provide the PPSP with additional information to approve the final site location (Fig. F5). The PPSP moved Site 1146 to *JOIDES Resolution* Leg 184, Line 3, at shotpoint 3241 (Fig. F11B).Total sediment thickness at the site is >1.4 s, with a prominent double reflector at ~0.77 s (Figs. F11A, F11B, F12). Several additional reflectors have been identified at Site 1146 and are thought to be regional in nature. A reflector at ~0.2 s was thought to be T_1, which lies near the Miocene/Pliocene boundary (~5.2 Ma); a double reflector at ~0.5 s was believed to be T_4, near the lower–middle Miocene boundary (15–16 Ma) (Ludmann and Wong, 1999). However, initial reflector assignments in the Leg 184 prospectus were uncertain, at best. The *JOIDES Resolution* 3.5-kHz data (Fig. F13) and SONNE95 PARASOUND data (Sarnthein et al., 1994) reveal relatively smooth sediment cover with indistinct overlapping hyperbole and parallel conformable sub-bottom reflectors.

Seismic and Sediment Stratigraphy

At Site 1146A, acoustical impedance was calculated over the downhole logged section (273 to 593 mbsf). Unfortunately, hole conditions necessitated lowering the drill string for the sonic log; therefore, in situ *P*-wave velocity data are not available for the upper section. We adjusted the physical properties core-log data for bulk density and *P*-wave velocity to give a continuous gradient the from core top to the logged interval (Fig. F14).

A summary of the depth/age relationships of the Site 1146 reflectors is given in Table T2. Reflector T_1 lies at ~0.2 s TWT at the base of a zone of strong reflectors extending from the surface to 0.2 s. This level is equivalent to ~150 mbsf and has an age of ~1.4 Ma. Hence, this reflector is more closely related to Reflector T_0 and is definitely not T_1. The double reflector thought to be T_4 coincides with a distinct minima in the acoustical impedance at ~0.50 s TWT. This level is equivalent to a depth of ~430 mbsf and an age of ~9.8 Ma. Thus, this reflector is equivalent to the middle/upper Miocene Reflector T_2 in the regional reflector stratigraphy (Ludmann and Wong, 1999). Given the velocity and age structure of Hole 1146A, if Reflector T_4 is 14 Ma, it would be expected to occur at ~0.59–0.60 s TWT at ~520–530 mbsf. This level lies near a minimum in the acoustical impedance, which increases downhole to the base of the section (Fig. F14). At ~530 mbsf, we observe a number of

F11. Single-channel seismic lines defining position of Site 1146, p. 24.
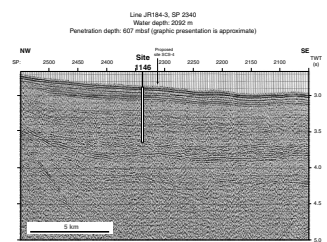
F12. Precruise seismic line across Site 1146, p. 26.
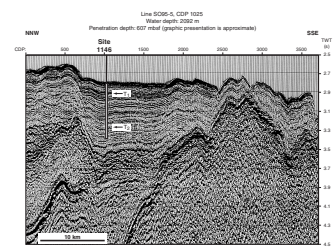
F13. 3.5-kHz records at Site 1146, p. 27.
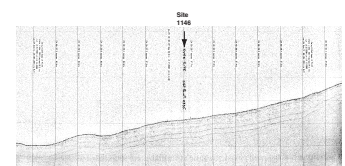
F14. Acoustical impedance record compared with seismic reflector stratigraphy, Site 1146, p. 29.
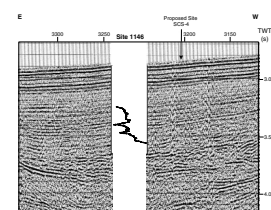
physical changes, including a decrease in linear sedimentation rates (LSR), a decrease in magnetic susceptibility, and an increase in natural gamma radiation (Fig. F17, p. 62, in the "Leg 184 Summary" chapter). However, a distinct reflector is not observed in the *JOIDES Resolution* seismic data. This level seems to fall within a layered sequence bounded by the more distinct reflectors at 0.5 and 0.7 s TWT. Perhaps additional postcruise processing and analysis will better resolve the T_4 reflector at Site 1146. A deeper series of reflectors, ranging from ~0.77 to ~0.97 TWT (Fig. F11), are estimated to be from 22 to 29 Ma based on downward continuation of velocities and LSRs at the base of the cored section.

The character of these reflectors suggests rapid infilling of a down-dropped block, which may have occurred in the early part of the SCS drift phase, which began at ~32 Ma. Even deeper reflectors at ~1.25 s TWT may be associated with the initiation of the drift phase and thus coincide with the T_7 reflector of Ludmann and Wong (1999). Unfortunately, these deeper reflectors are outside our recovered section, and we cannot make reliable estimates of their exact depth and age.

Sites 1147 and 1148 (SCS-5C)

Site 1147 is located at 18°50.11′N, 116°33.28′E, at a water depth of 3246 m. Site 1148 is located at 18°50.17′N, 116°33.94′E, at a water depth of 3294 m. Site 1148 was initially designated as SCS-5C, near the base of the continental slope on seismic Line SONNE95-5 at CDP 7500 (Figs. F5, F15). The *JOIDES Resolution* acquired crossing seismic lines as part of the survey required for final site approval. The PPSP evaluation of the new seismic data moved the final Site 1148 location to *JOIDES Resolution* 184, Line 1, at shotpoint 1980 ~1.05 nmi east of the proposed site SCS-5C (see Fig. F18, p. 63, in the "Leg 184 Summary" chapter; Figs. F5, F16B). Site 1148 was cored to 853 mbsf, which was thought to penetrate the strong reflector sequence at ~0.85–~0.90 s TWT. Initially, this reflector was described as acoustical basement and was believed to represent the prespreading (and possibly the prerifting) surface. Initial interpretation of the SONNE95 seismic stratigraphy identified Reflector T_1 (top of Miocene, 5.2 Ma) at ~0.2 s subsurface and Reflector T_7 (mid-Oligocene, ~30 Ma) at ~0.52 s subsurface (Fig. F15). These same reflectors are clear in the *JOIDES Resolution* seismic lines (Fig. F16A, F16B), but their age assignments are somewhat in doubt.

The *JOIDES Resolution* 3.5-kHz data (Fig. F17) and SONNE95 PARA-SOUND data (Sarnthein et al., 1994) revealed relatively smooth draped sediment cover with parallel conformable sub-bottom reflectors. The 3.5-kHz data disclosed a surface slump scar at the proposed location of Site 1148 (Fig. F17A, F17B). As a result of these data, Site 1147 was located upslope from the slump to obtain a complete upper sediment section.

Seismic and Sediment Stratigraphy

The wireline logs of Site 1148 enabled construction of acoustical impedance over the interval from ~200 to ~698 mbsf. We used the physical properties core-log data for bulk density and *P*-wave velocity and adjusted them to calculate the TWT of the top of the logged interval. Below the logged interval (698 to 850 mbsf), we used the physical properties and downward continuation of the velocity model to estimate the TWT depth. On the basis of in situ velocity logs from Site

F15. Precruise seismic line across Site 1148, p. 30.
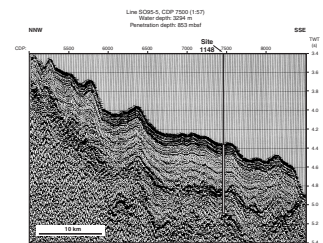
F16. *JOIDES Resolution* Leg 184 seismic lines defining positions of Sites 1147 and 1148, p. 31.
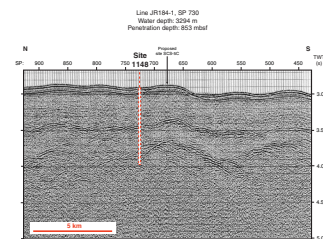
F17. 3.5-kHz records at Sites 1147 and 1148, p. 33.
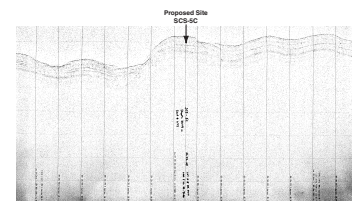
1148, the 700 (Hole 1148A) and 859 mbsf (Hole 1148B) penetration is equivalent to ~0.78 and ~0.91 s TWT, respectively.

The acoustical impedance log shows a continuous increase in impedance from the top of the logged interval to 450 mbsf, where it first increases rapidly and then decreases abruptly. This strong impedance contrast coincides with the strong reflector at 0.52 s (Fig. F18) and has an age of ~22.6 Ma. Hence, this major reflector is younger than the lower Oligocene Reflector T_7 (32 Ma) but is older than the widely observed lower/middle Miocene Reflector T_4 (14 Ma). The age of this feature seems most consistent with the T_5 boundary of Chen et al. (1987) but is still somewhat younger than their designation of 26.2 Ma. Following this reflector, acoustical impedance continuously increases downhole with a small reversal at the base of the section. The "basement" reflector at ~0.9 s was projected to occur at ~800 mbsf. Although drilling slowed at this level, no other evidence of a change in composition or properties occurred at this depth. The age of the interval from 800 to 850 mbsf is ~31.5 to ~31.8 Ma. It is therefore close in age to the lower Oligocene Reflector T_7, which is thought to mark the breakup and transition from the rifting to the spreading phase. In well records on the continental shelf near the Pearl River Mouth Basin, this basement reflector was believed to mark the termination of Paleogene syn-rift sedimentation in midslope half-grabens (Ru et al., 1994). Major depositional hiatuses have been observed on the shelf in the lower part of the lower Miocene, near the end of the middle Miocene, and around the Pliocene/Pleistocene boundary (L. Huang, pers. comm., 1998; Ludmann and Wong, 1999). Although Site 1148 penetrated the section that should contain Reflectors T_1, T_2, and T_4, the latter two do not seem to be well developed in this deep-water section. Perhaps further processing of the seismic lines will help define these Neogene reflectors.

Summary

The sequence of reflectors observed in the seismics and cored during Leg 184 was highly variable. Although some of the features observed in the Pearl River Mouth Basin (Ludmann and Wong, 1999) were observed at our offshore sites, their manifestation varied greatly between sites (Table T2). Both of the eastern high-accumulation sites (1144 and 1145) seem to record a mid-Pleistocene event, which is not readily observed at the western sites (1146 and 1148). However, within the preliminary dating, a Pliocene/Pleistocene reflector seems common to the northern sites, except for Site 1148. Although Sites 1143 and 1146 share a nominal T_2 reflector, the older features are more variable and have possible multiple g reflectors. The extrapolation of depth/age at Site 1146 indicates that the reflectors at 0.77 to 0.80 s are consistent with (but somewhat younger than) the age of the T_5 Oligocene/Miocene reflector and are the same age as the well-dated reflector at 0.52 s at Site 1148. The basal reflectors at Site 1148 seem to correlate roughly with the T_7 reflector, which is thought to mark the initiation of seafloor spreading in the SCS. Although the identification of the Pearl River Mouth Basin reflector sequences in the South China Sea deep-sea sediments is tantalizing and intriguing, much detailed work is necessary to refine the velocity and age models to more rigorously test the temporal and spatial connections between the shelf and the continental margin sediments of the SCS.

F18. Acoustical impedance record compared with seismic reflector stratigraphy, Site 1148, p. 35.
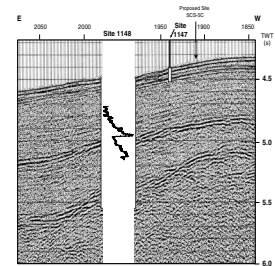
REFERENCES

Briais, A., Patriat, P., and Tapponnier, P., 1993. Updated interpretation of magnetic anomalies and seafloor spreading stages in the South China Sea: implications for the Tertiary tectonics of Southeast Asia. *J. Geophys. Res.,* 98:6299–6328.

Chen, S., Li, Z., and Zhou, Y., 1987. Major oil accumulation characteristics and exploration direction in the Pearl River Mouth Basin. *China Oil,* Winter:17–23.

Comas, M.C., Zahn, R., Klaus, A., et al., 1996. *Prod. ODP, Init. Repts.,* 161: College Station, TX (Ocean Drilling Program).

Damuth, J.E., 1979. Migrating sediment waves created by turbidity currents in the northern South China Basin. *Geology,* 7:520–523.

————, 1980a. Quaternary sedimentation processes in the South China basin as revealed by echo-character mapping and piston-core studies. *In* Hayes, D.E. (Ed.), *The Tectonic and Geologic Evolution of the Southeast Asian Seas and Islands.* Geophys. Monogr., Am. Geophys. Union, 23:105–125.

————, 1980b. Use of high-frequency (3.5–12 kHz) echograms in the study of near-bottom sedimentation processes in the deep-sea: a review. *Mar. Geol.,* 38:51–75.

Guong, Z., Jin, Q., Qui, Z., Wang, S., and Meng, J., 1989. Geology, tectonics, and evolution of the Pearl River Mouth Basin. *In* Zhu, X. (Ed.), *Chinese Sedimentary Basins:* Amsterdam (Elsevier), 181–196.

Jiang, Z., Lin, Z., Li, M., et al., 1994. *Tertiary in Petroliferous Regions of China, VIII. The North Continental Shelf Region of South China Sea:* Beijing (Petroleum Industry Press). (in Chinese)

Ludmann, T., and Wong, H.K., 1999. Neotectonic regime on the passive continental margin of the northern South China Sea. *Tectonophysics,* 311:113–138.

Ru, K., Di, Z., and Chen, H.-Z.,1994. Basin evolution and hydrocarbon potential of the northern South China Margin. *In* Di, Z., et al. (Eds.), *Oceanology of China Seas,* 2:361–372.

Sarnthein, M., Pflaumann, U., Wang, P.X., and Wong, H.K. (Eds.), 1994. Preliminary Report on Sonne-95 Cruise "Monitor Monsoon" to the South China Sea. *Rep. Geol.-Palaontol. Inst. Univ. Kiel.,* 68.

Taylor, B., and Hayes, D.E., 1983. Origin and history of the South China Sea Basin. *In* Hayes, D.E. (Ed.), *Tectonic and Geologic Evolution of Southeast Asian Seas and Islands* (Pt. 2). Geophys. Monogr., Am. Geophys. Union, 27:23–56.

Wong, H.K., Ludmann, T., and Wollschlager, M., 1994. Seismic reflection profiling at the northern Continental Margin of the South China Sea (SONNE-95 Cruise). *In* Sarnthein, M., Pflaumann, U., Wang, P.X., and Wong, H.K. (Eds.), *Preliminary Report on Sonne-95 Cruise "Monitor Monsoon" to the South China Sea.* Rep. Geol.-Palaontol. Inst. Univ. Kiel, 68.

Wu, S., Wong, H.K., and Ludmann, T., 1999. Gravity-driven sedimentation on the northwestern continental slope in the South China sea: results from high-resolution seismic data and piston cores. *Chin. J. Oceanol. Limnol.,* V17-2:155–169.

Figure F1. Precruise Guangzhou Marine Geology Survey seismic survey Lines NS95-240 and NSL95-160 in the southern South China Sea showing the location of Site 1143. The *JOIDES Resolution* Leg 184 3.5-kHz record across Site 1143 overlies the NSL95-160 line.
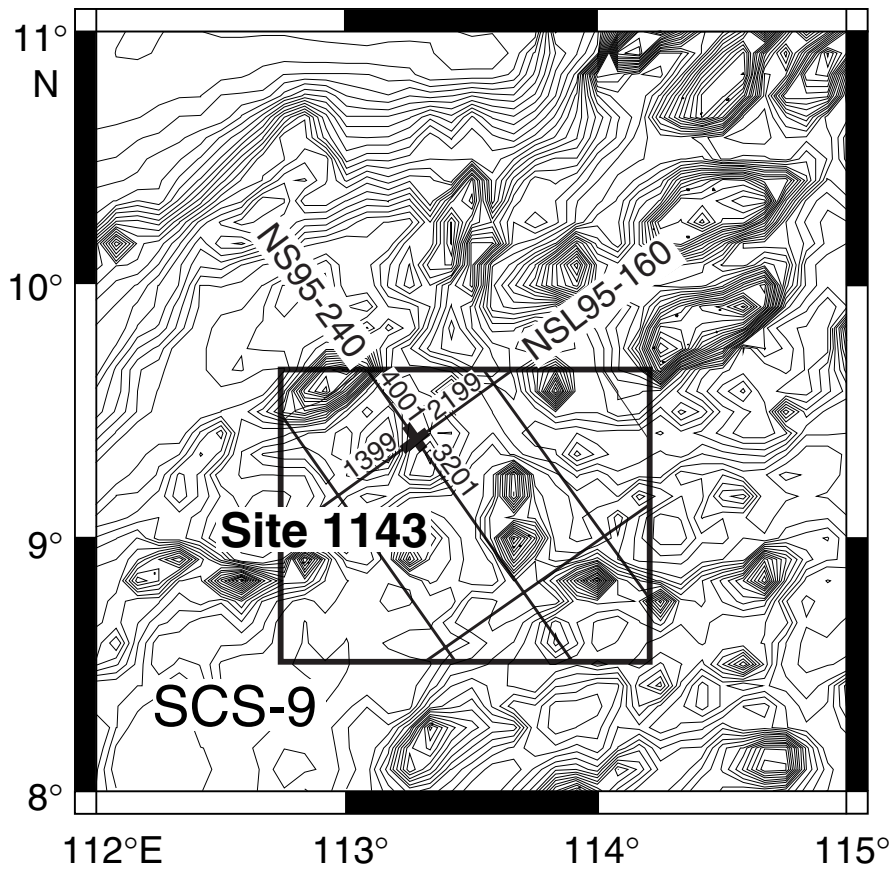
Figure F2. A. Guangzhou Marine Geology Survey multichannel seismic lines that locate Site 1143 (proposed site SCS-9) at the crossing points of Line NS95-240 (CDP 3617) and Line NSL95-160 (CDP 1812). Line NS95-240 is shown below. TWT = two-way traveltime. (Continued on next page.)

Line NS95-240, CDP 3617
Water depth: 2772 m
Penetration depth: 500 mbsf (graphic presentation is approximate)
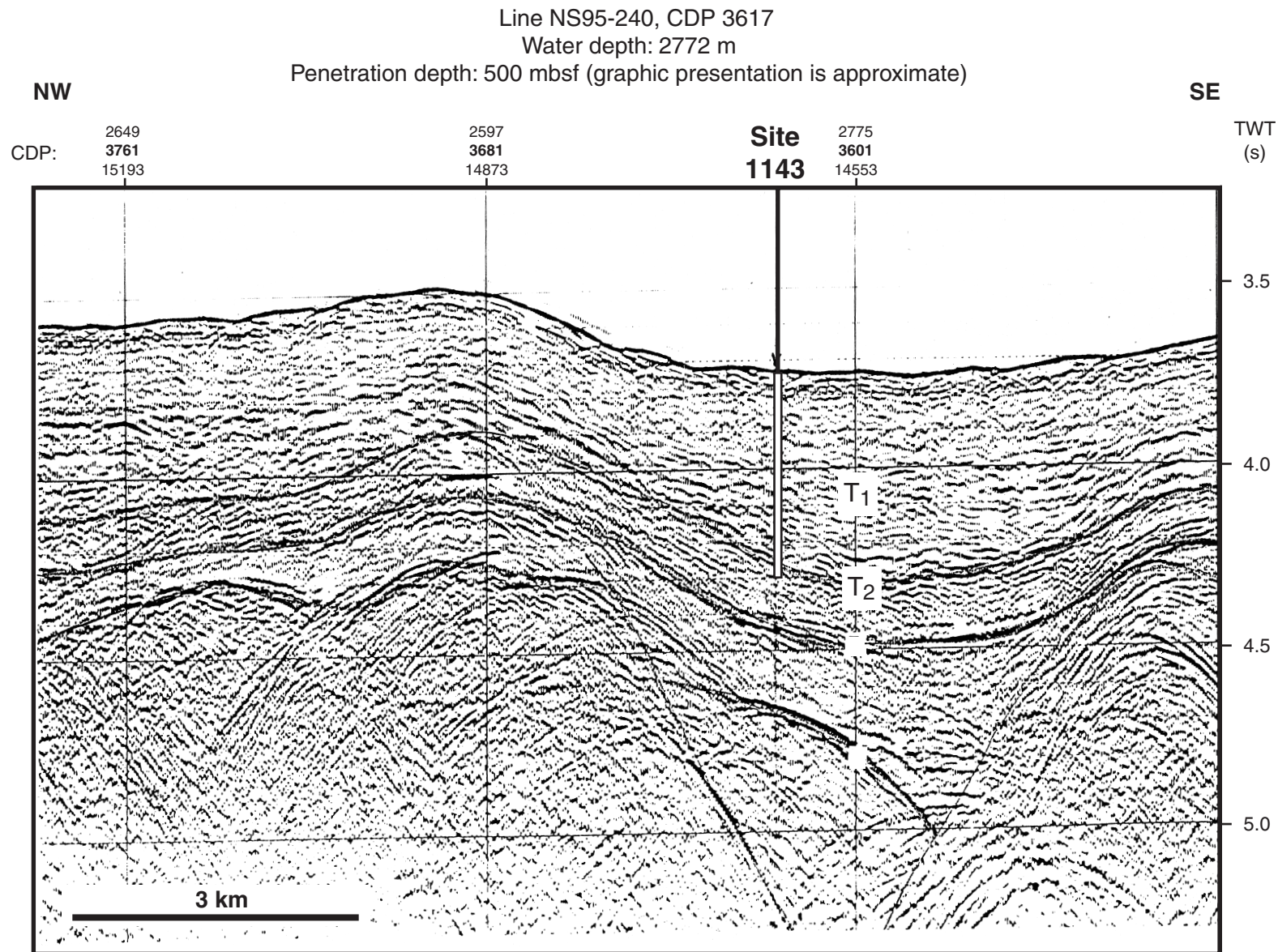
Figure F2 (continued). B. Guangzhou Marine Geology Survey multichannel seismic lines that locate Site 1143 (proposed site SCS-9) at the crossing points of Line NS95-240 (CDP 3617) and Line NSL95-160 (CDP 1812). Line NSL95-160 is shown below.

Line NSL95-160, CDP 1812
Water depth: 2772 m
Penetration depth: 500 mbsf (graphic presentation is approximate)
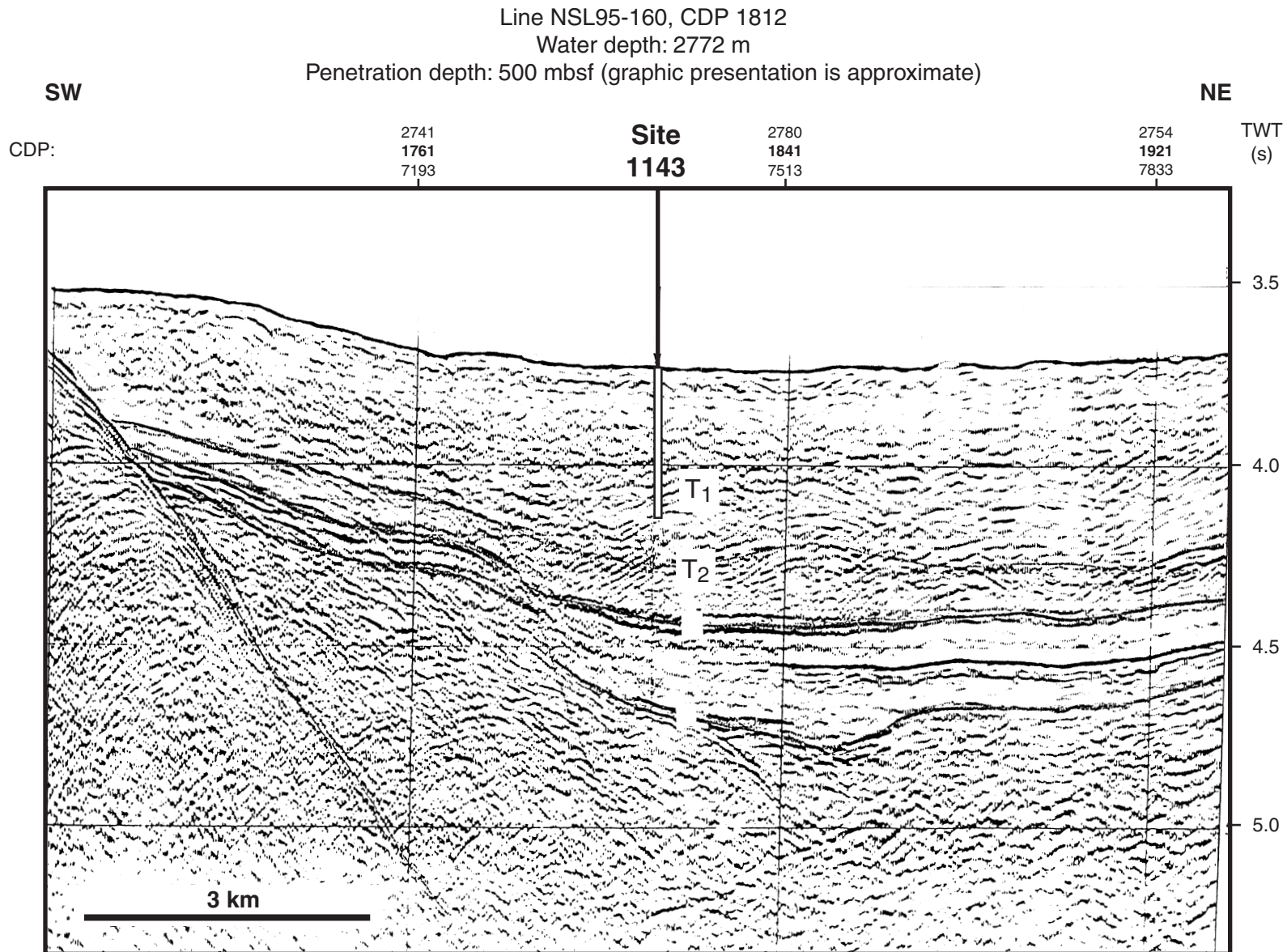
Figure F3. A. The *JOIDES Resolution* Leg 184 3.5-kHz record on approach and across Site 1143. This track follows the SO95 Line 160 from southwest to northeast and is ~15 nmi long (0550–0655 hr, 3/3/99). (Continued on next page.)

Figure F3 (continued). B. A continuation of the JR 3.5-kHz record across Site 1143 (0655–0755 hr, 3/3/99).
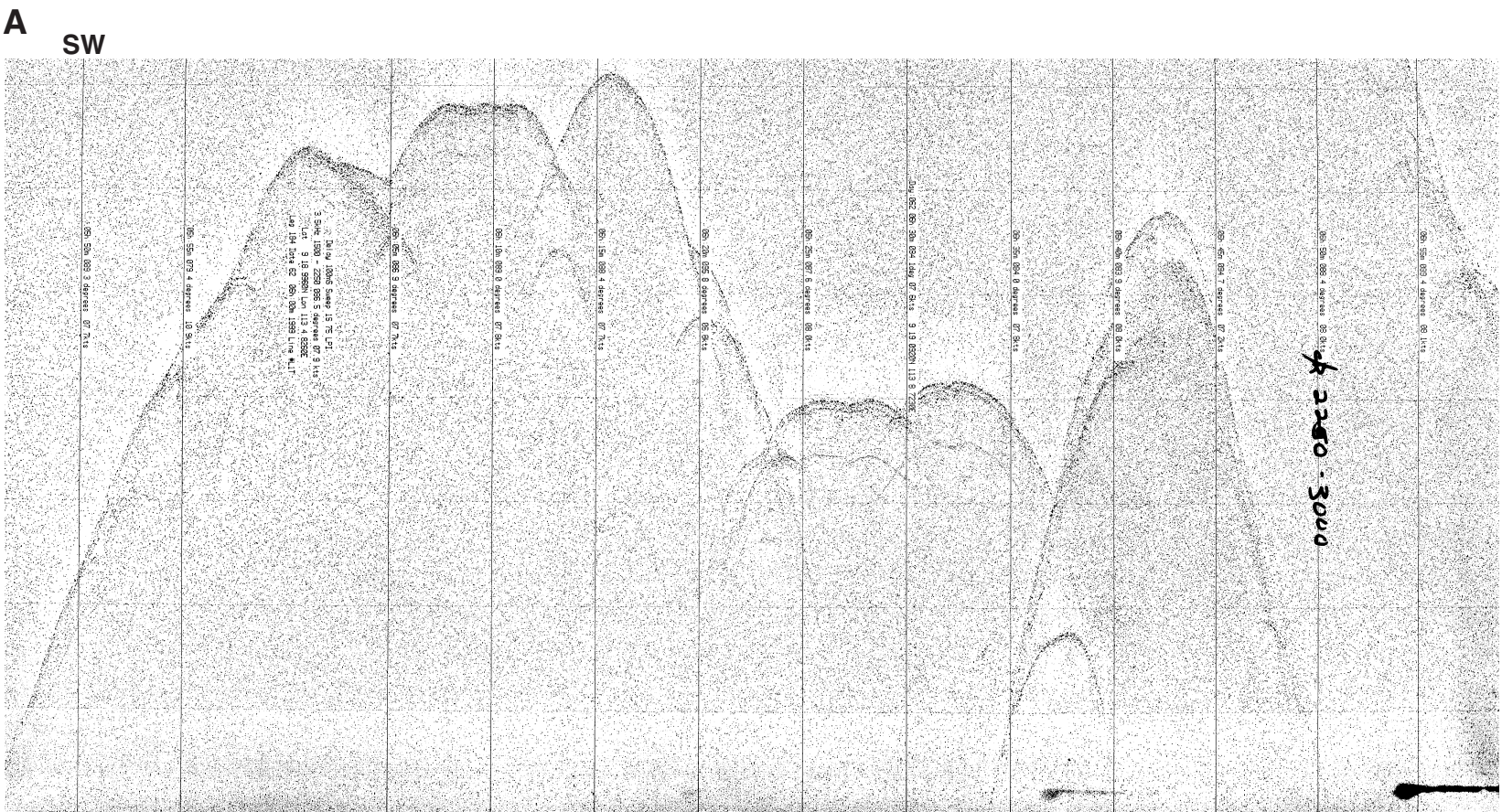
Figure F4. Comparison of the acoustical impedance record with seismic reflection stratigraphy (GMGS Line NS95-240) at Site 1143. TWT = two-way traveltime.
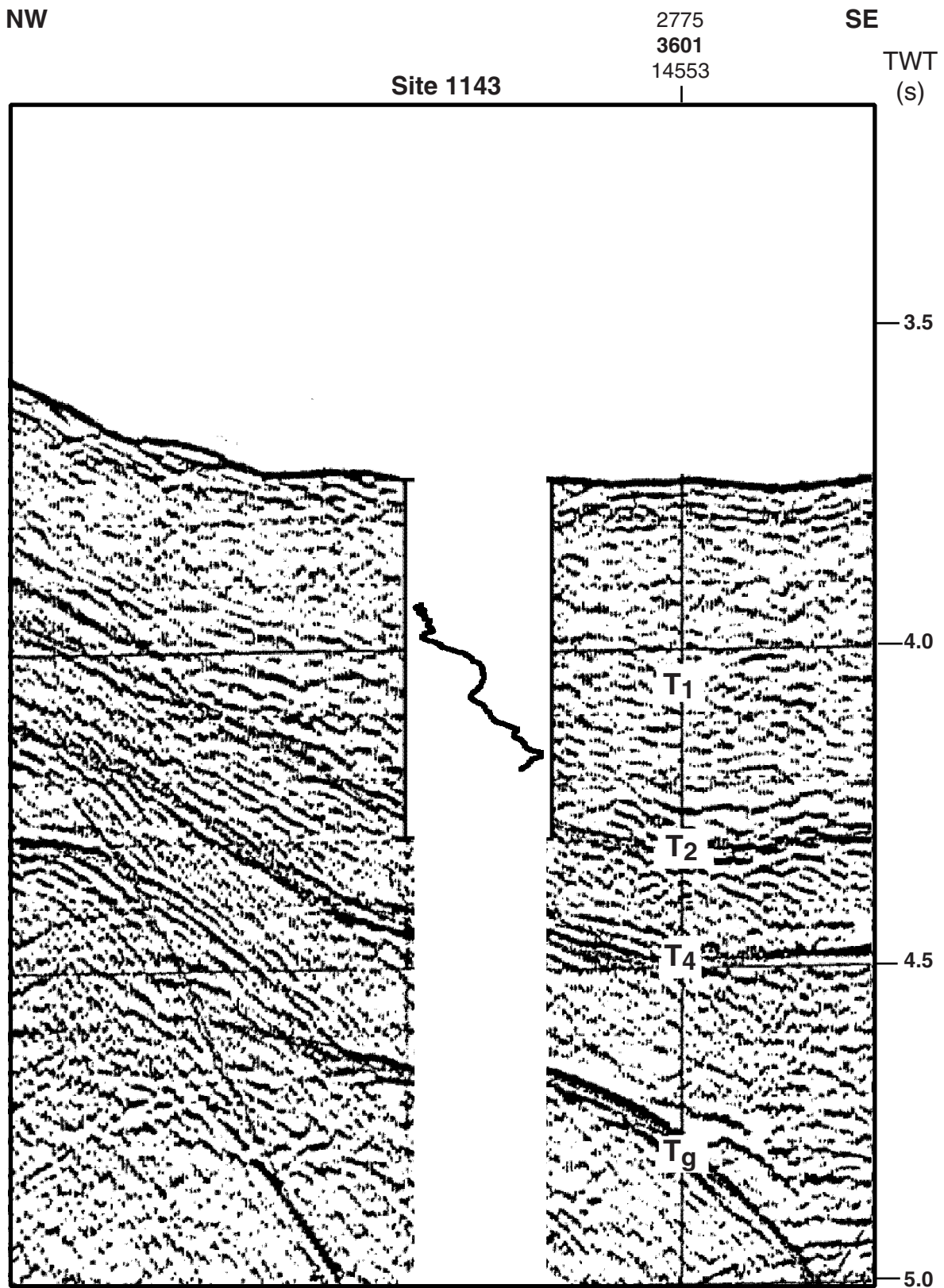
Figure F5. Precruise seismic survey lines and *JOIDES Resolution* Leg 184 survey lines in the northern South China Sea showing the locations of Sites 1144, 1145, 1146, 1147, and 1148 and of proposed sites that were not drilled.
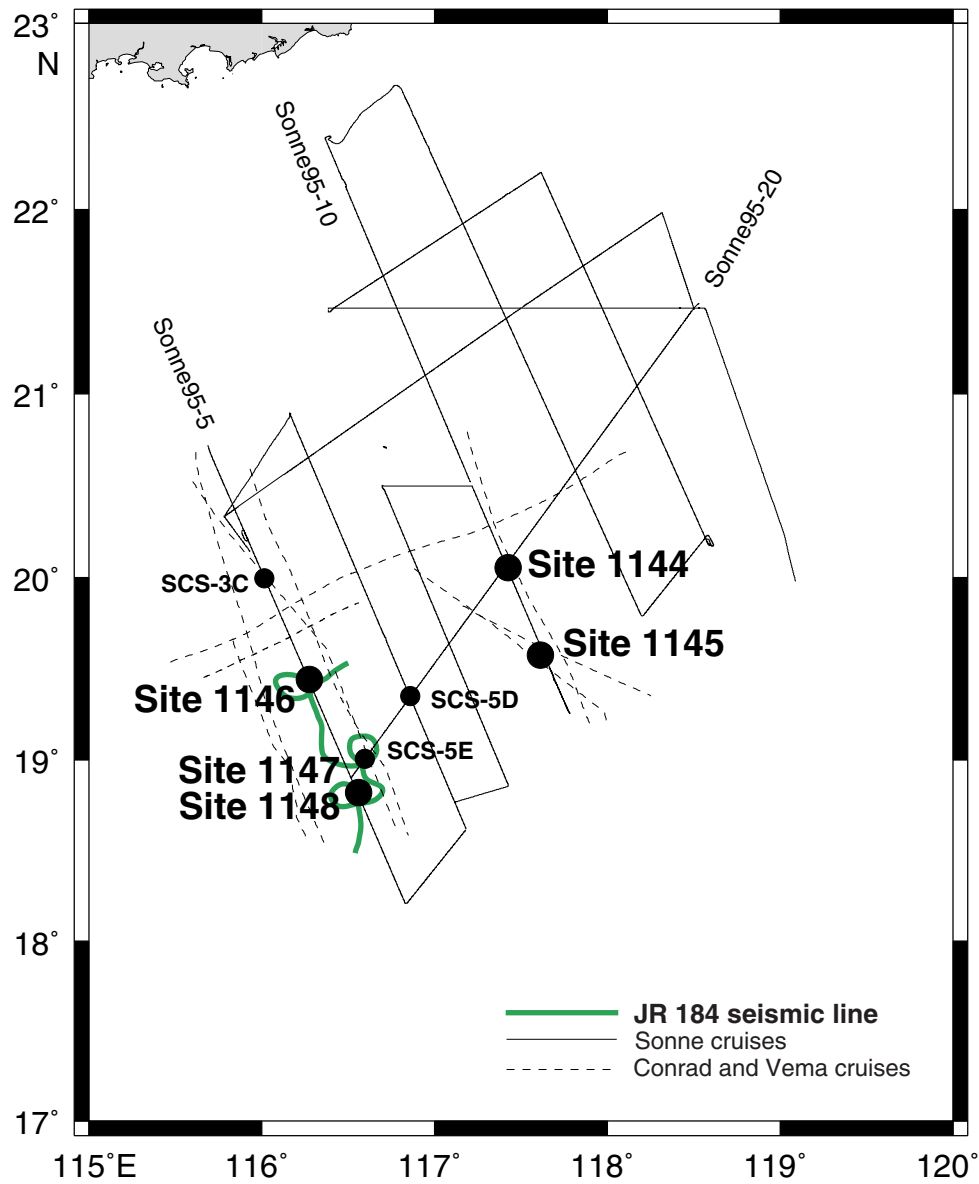
Figure F6. A. SONNE95 multichannel seismic lines that locate Site 1144 (proposed site SCS-1) at the crossing points of SONNE95, Line 10 (CDP 9700); and SONNE95, Line 20 (CDP 3430). Line 10 is shown below. TWT = two-way traveltime. (Continued on next page.)

Line SO95-10, CDP 9700 (4:20)
Water depth: 2037 m
Penetration depth: 453 mbsf (graphic presentation is approximate)
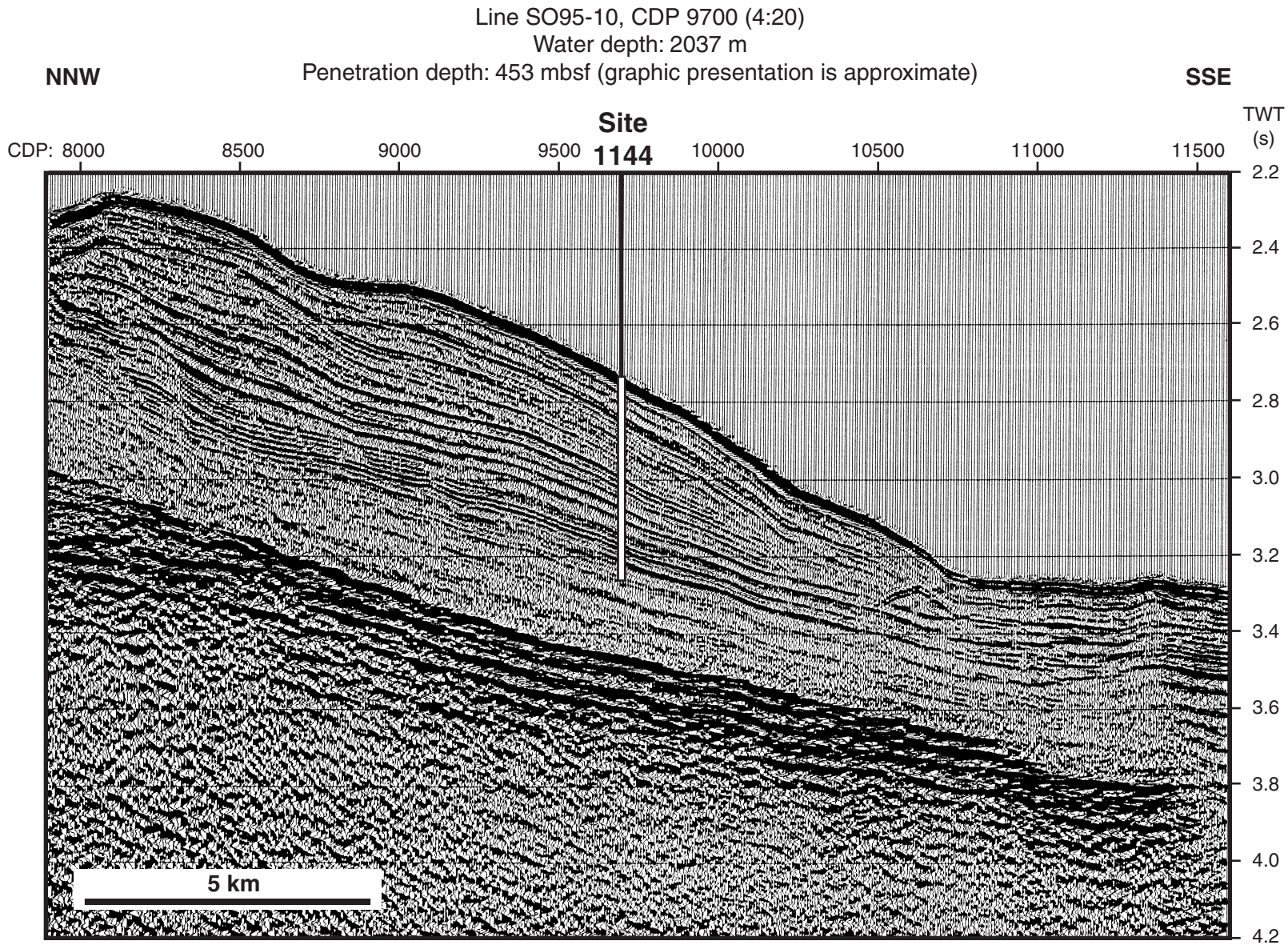
Figure F6 (continued). B. SONNE95 multichannel seismic lines that locate Site 1144 (proposed site SCS-1) at the crossing points of SONNE95, Line 10 (CDP 9700); and SONNE95, Line 20 (CDP 3430). Line 20 is shown below (Site 1144 is projected).

Line SO95-20, CDP 3430 (4:02)
Water depth: 2037 m
Penetration depth: 453 mbsf (graphic presentation is approximate)

Figure F7. The *JOIDES Resolution* Leg 184 3.5-kHz records on approach to Site 1144.
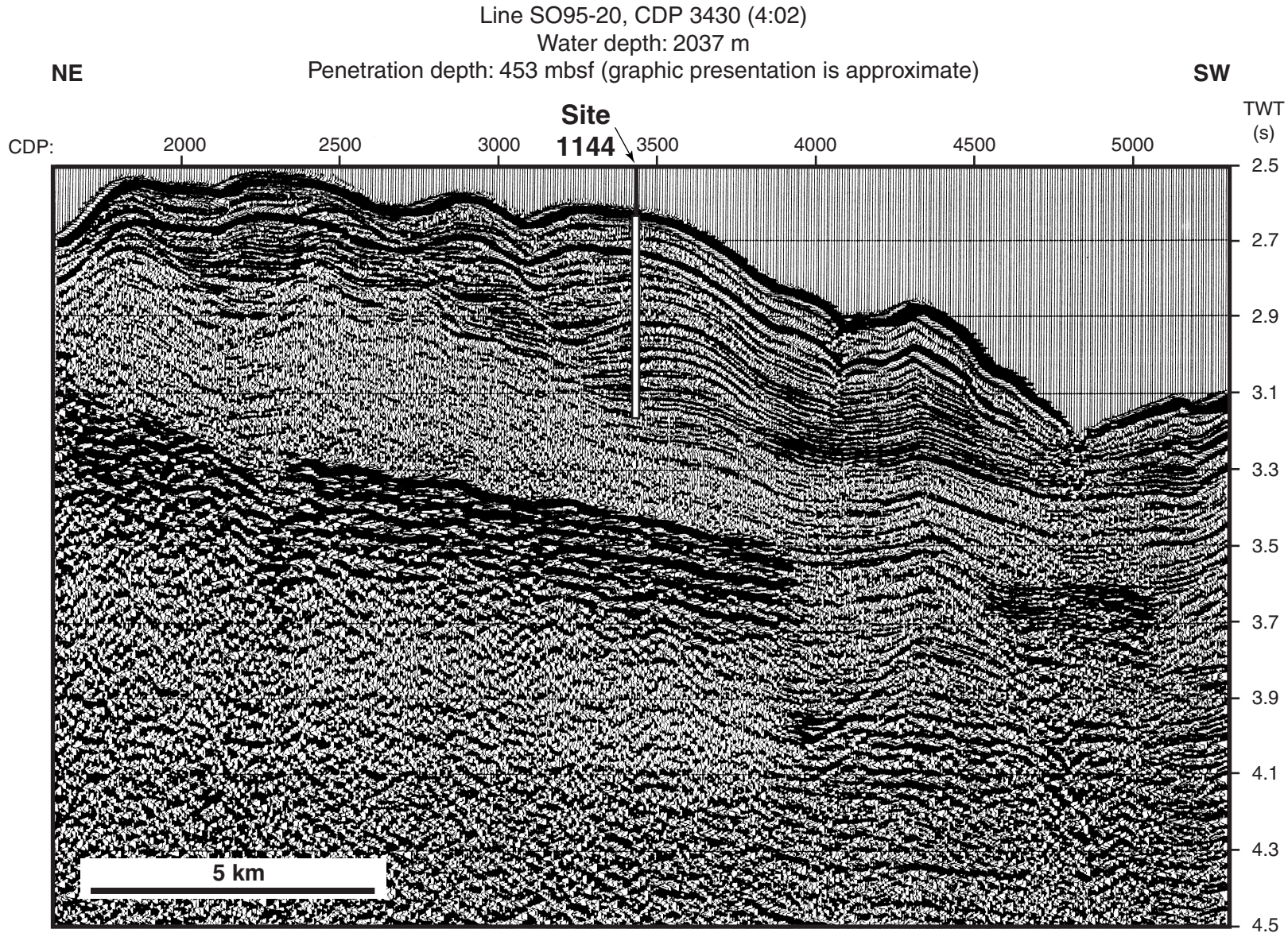
Figure F8. Comparison of the acoustical impedance record with seismic reflection stratigraphy (SONNE95, Line 10) at Site 1144. TWT = two-way traveltime.
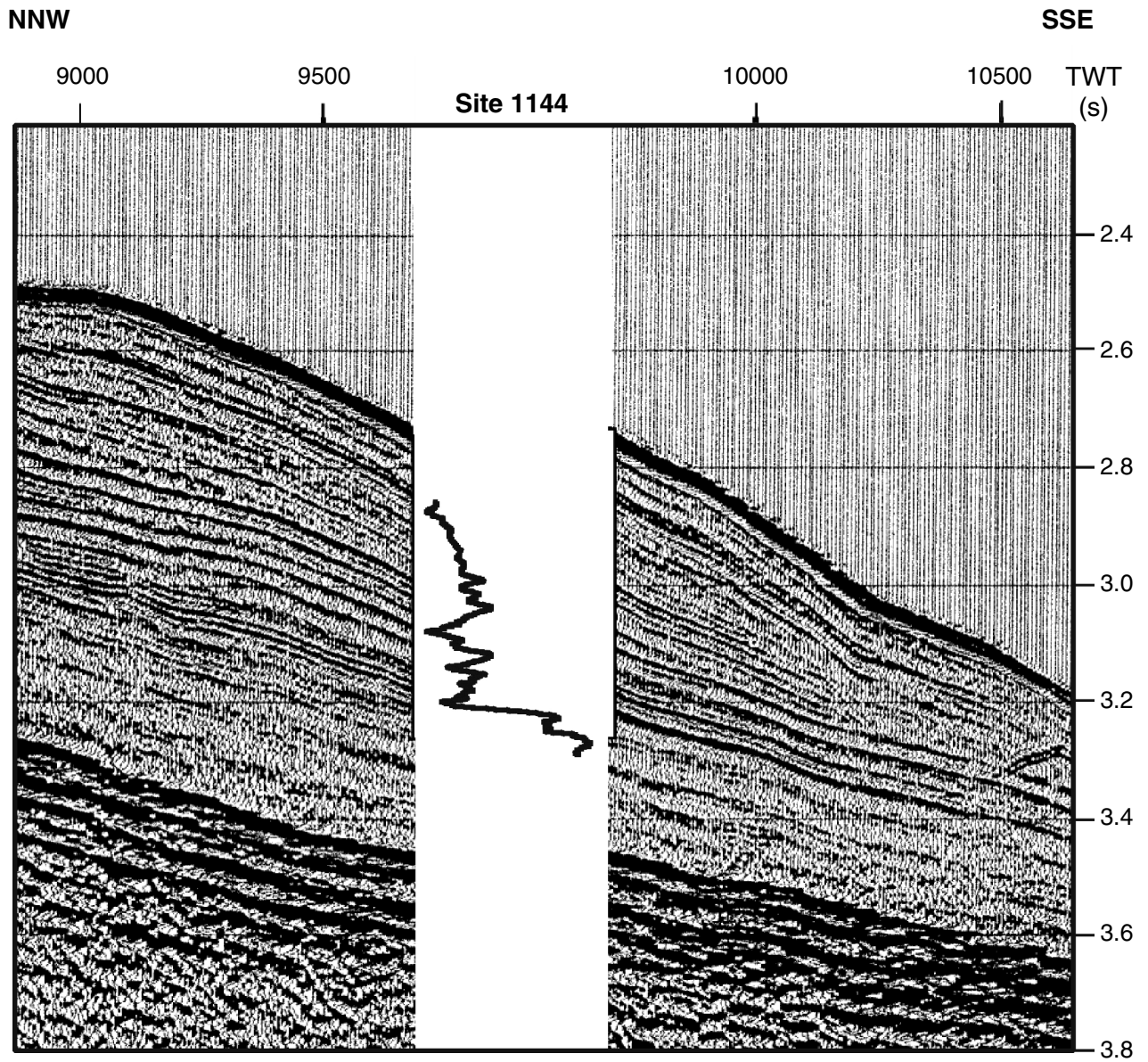
Figure F9. SONNE95 multichannel seismic line that defines Site 1145 (proposed site SCS-2) at SONNE95, Line 10 (CDP 4680). TWT = two-way traveltime.

Line SO95-10, CDP 4680 (11:10)
Water depth: 3175 m
Penetration depth: 200 mbsf (graphic presentation is approximate)
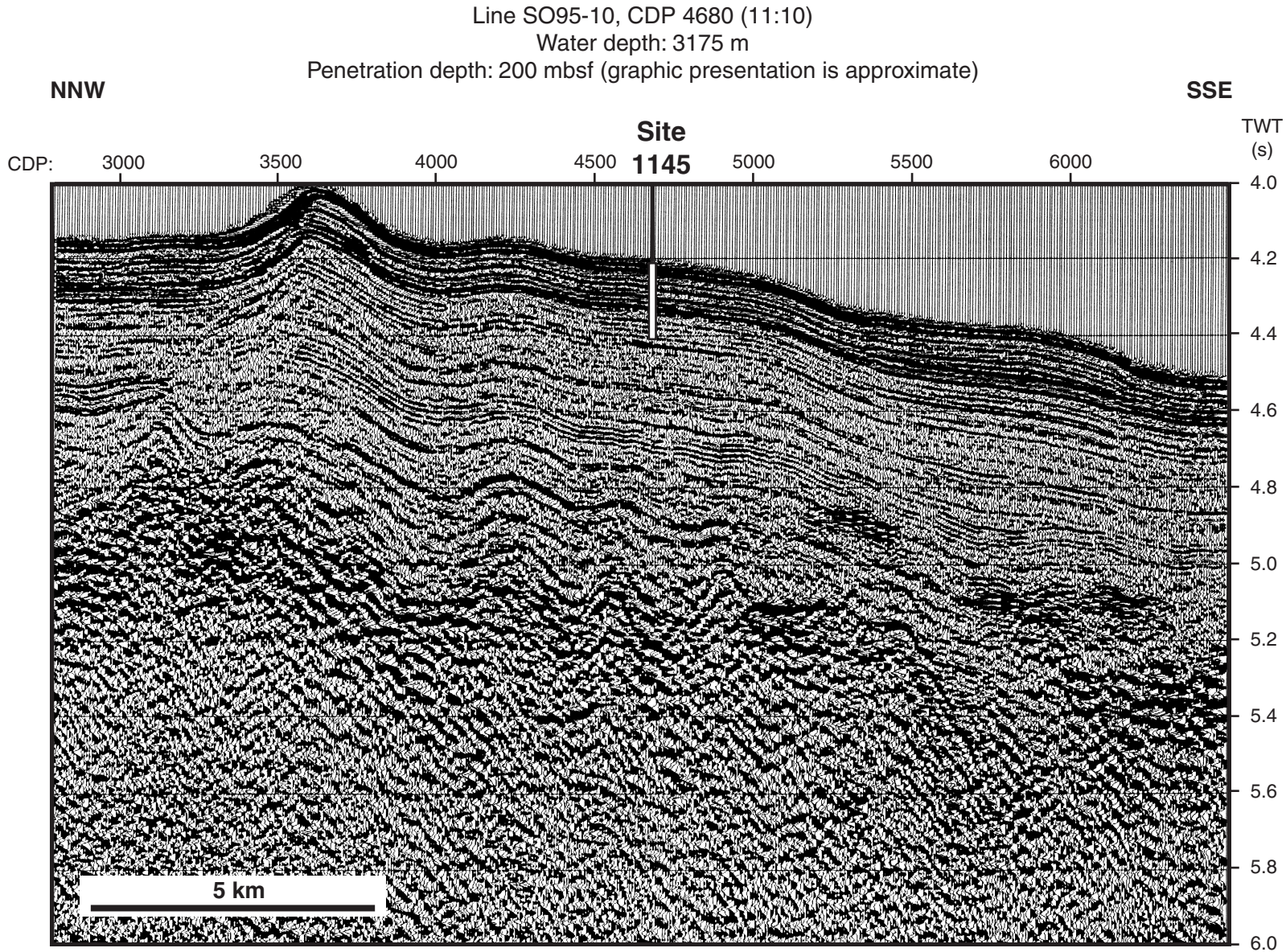
Figure F10. The *JOIDES Resolution* Leg 184 3.5-kHz records departing Site 1145.
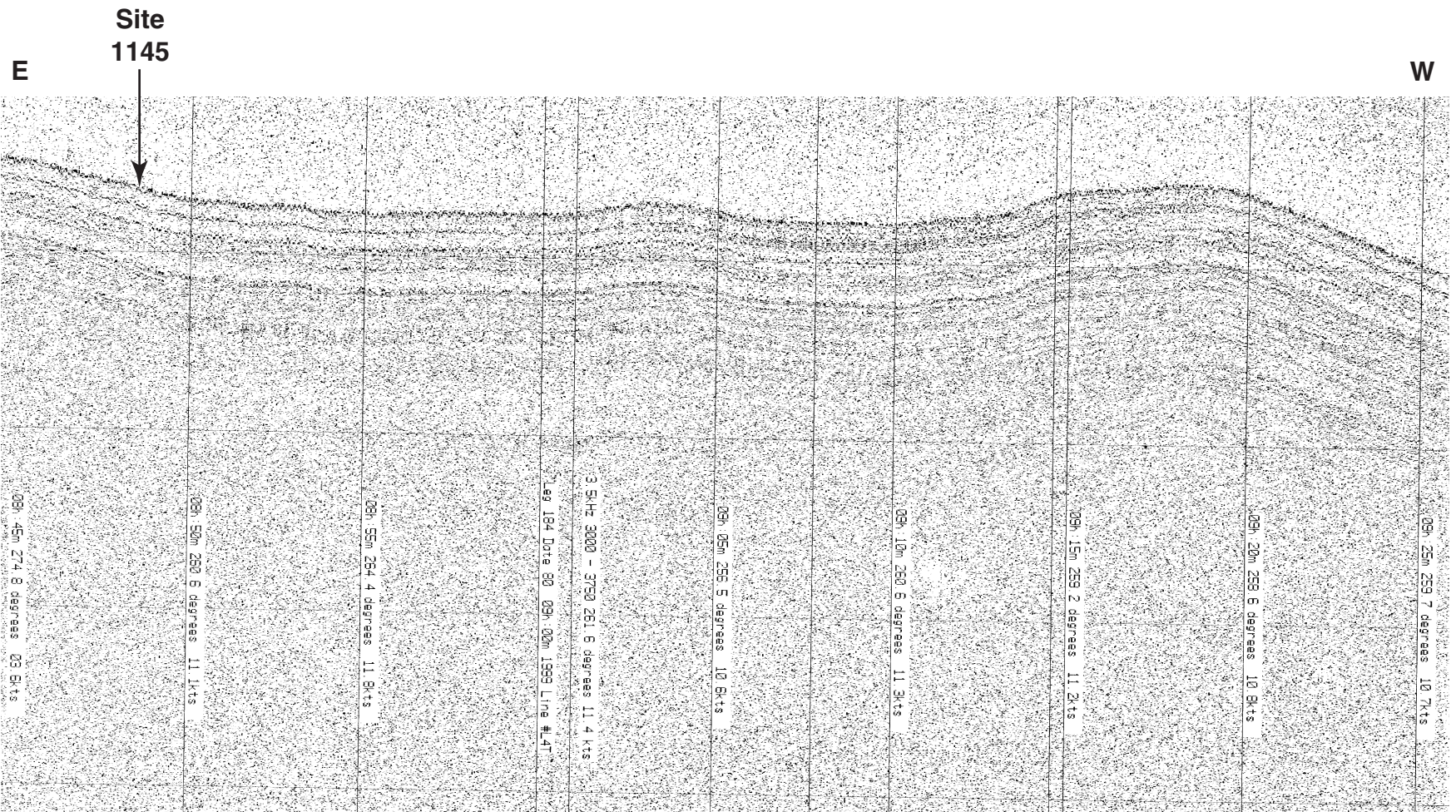
Figure F11. A. *JOIDES Resolution* Leg 184 single-channel seismic lines used to define the final location of Site 1146 near *JOIDES Resolution* (JR) Leg 184, Line 3 (SP 2340) and *JOIDES Resolution* (JR) Leg 184, Line 3 (SP 3240). Line JR184-3, SP 2340, is shown below. TWT = two-way traveltime. (Continued on next page.)

Line JR184-3, SP 2340
Water depth: 2092 m
Penetration depth: 607 mbsf (graphic presentation is approximate)
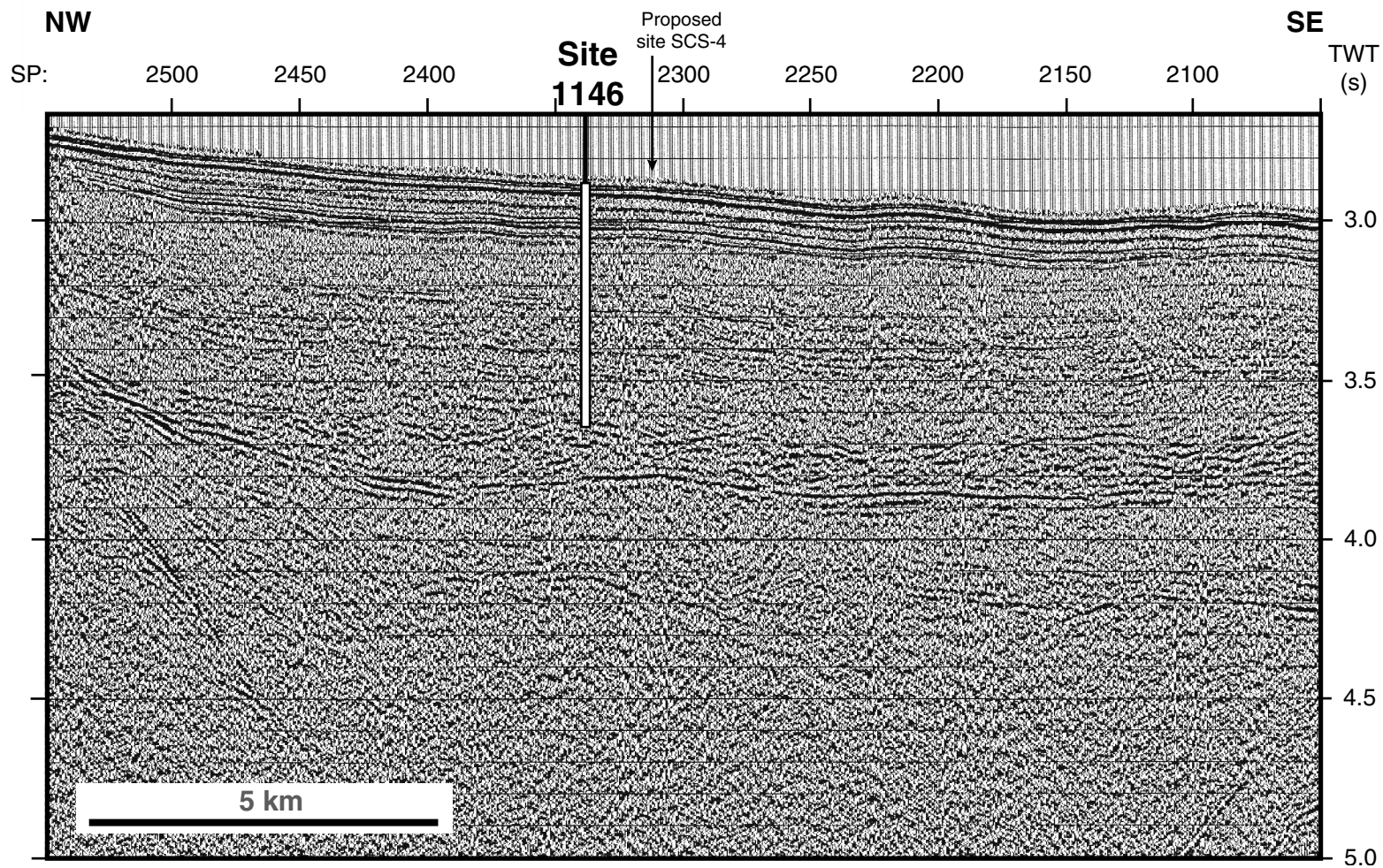
Figure F11 (continued). B. *JOIDES Resolution* Leg 184 single-channel seismic lines used to define the final location of Site 1146 near *JOIDES Resolution* (JR) Leg 184, Line 3 (SP 2340) and *JOIDES Resolution* (JR) Leg 184, Line 3 (SP 3240). Line JR184-3, SP 3240, is shown below.

Line JR184-3, SP 3240
Water depth: 2092 m
Penetration depth: 607 mbsf (graphic presentation is approximate)
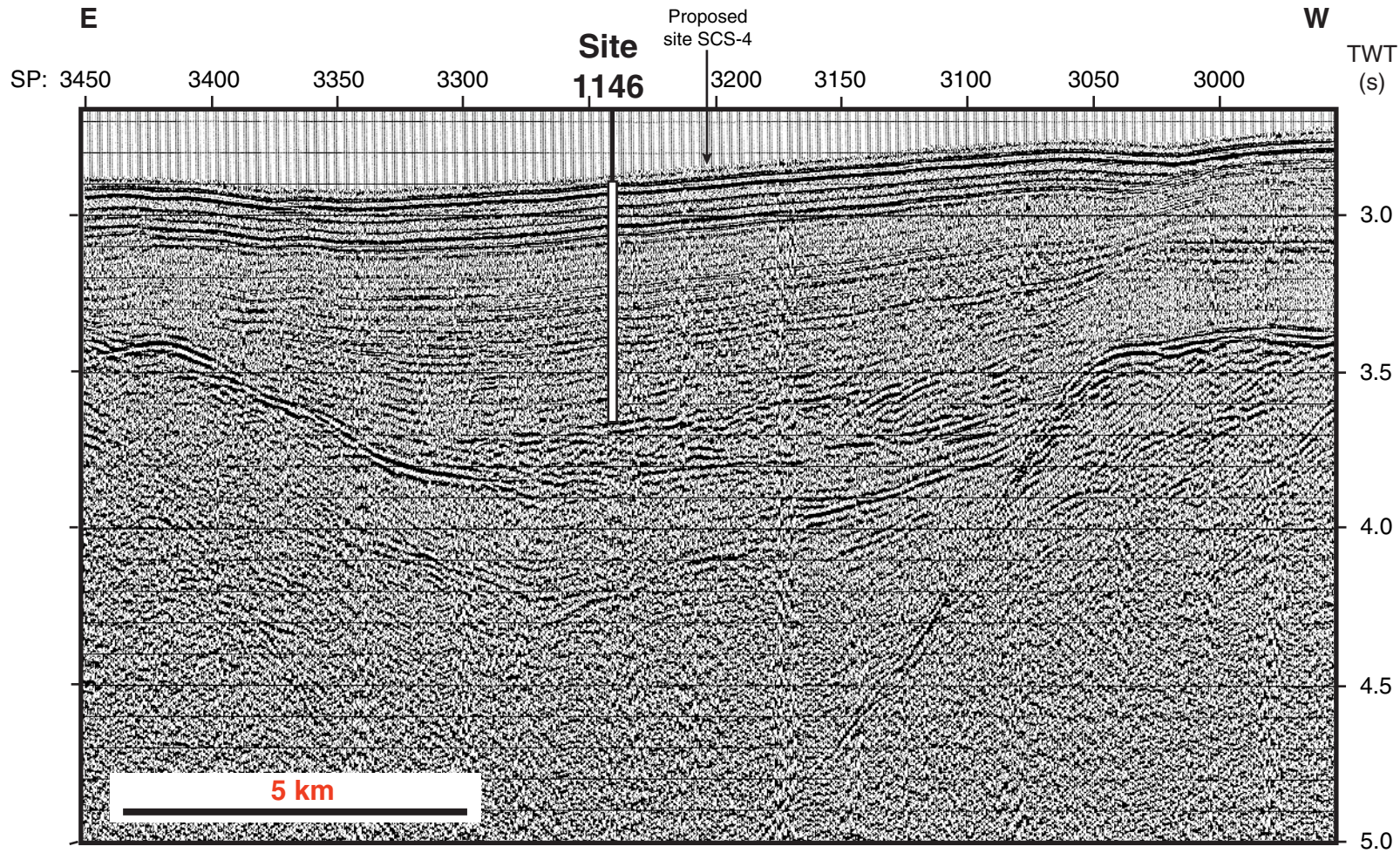
Figure F12. SONNE95 multichannel seismic line that defines Site 1146 (proposed site SCS-4) at SONNE95, Line 5 (CDP 1025). TWT = two-way traveltime.

Figure F13. The *JOIDES Resolution* Leg 184 3.5-kHz records across Site 1146. **A.** *JOIDES Resolution* Leg 184, Line 3 (JD71, 2300–2400 hr). JD = Julian day. (Continued on next page.)

Figure F13 (continued). B. *JOIDES Resolution* Leg 184, Line 3 (JD72, 0130–0230 hr).
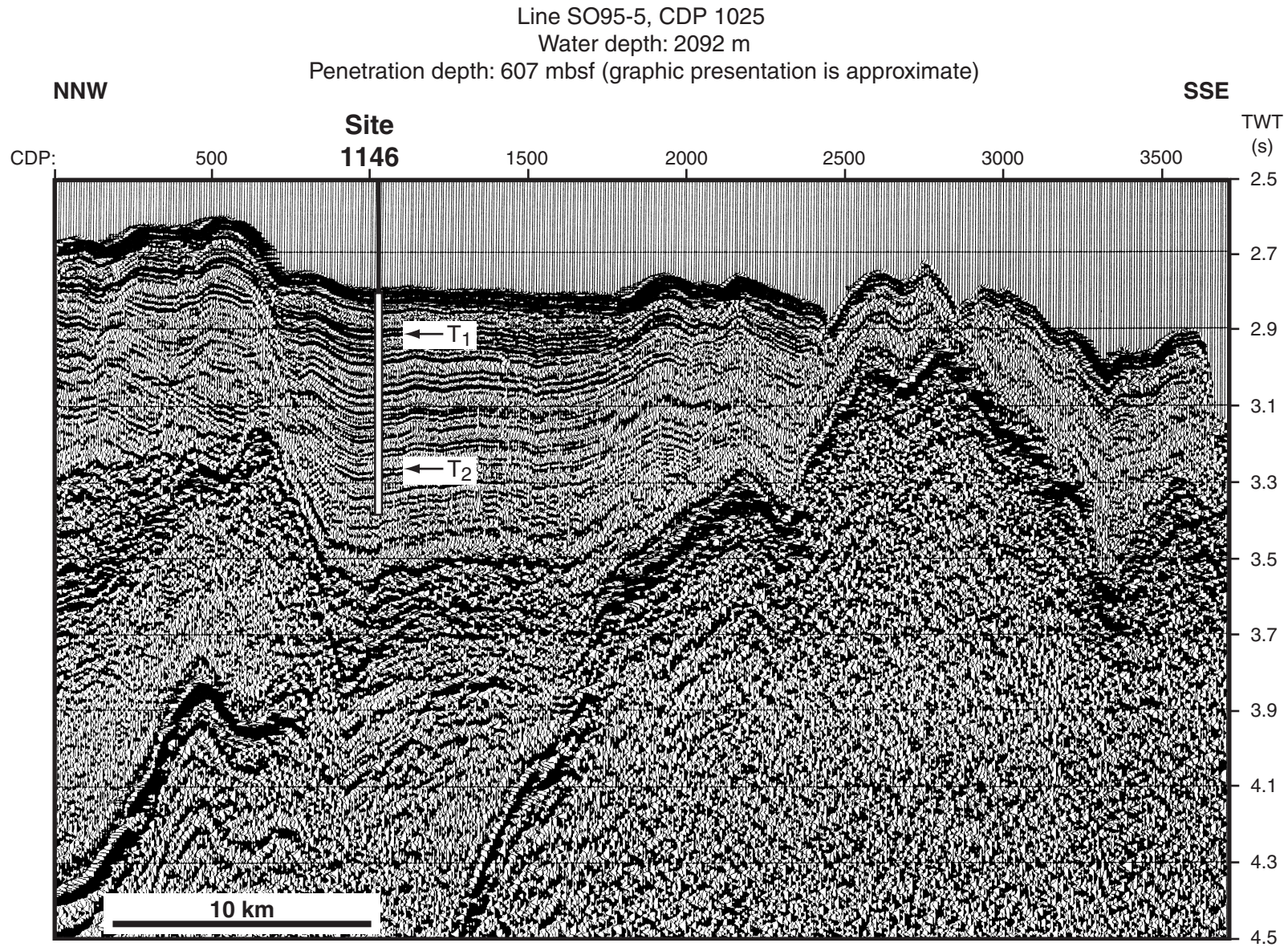
**Site
1146**

Figure F14. Comparison of the acoustical impedance record with seismic reflector stratigraphy (*JOIDES Resolution* Leg 184, Line 3) at Site 1146. TWT = two-way traveltime.
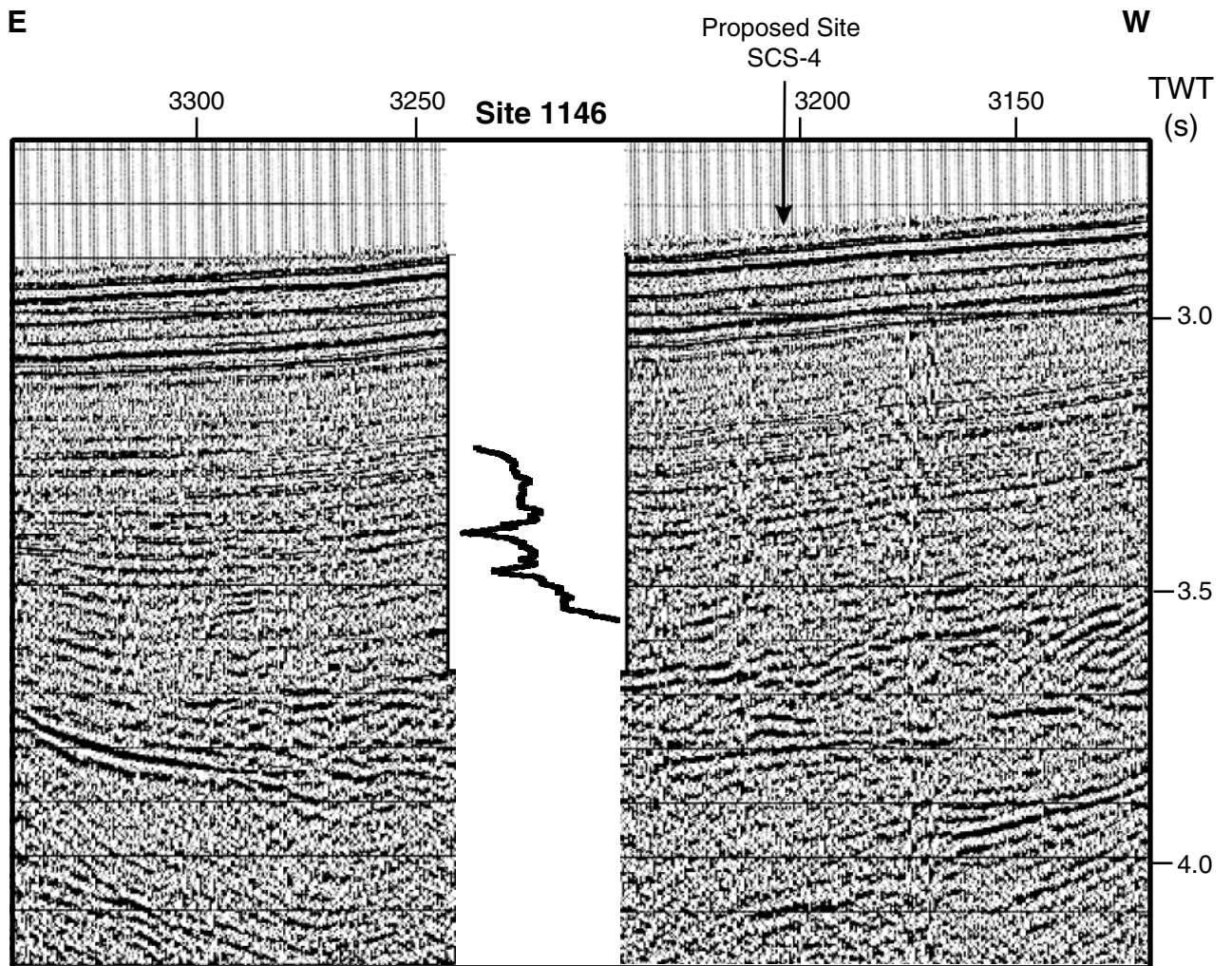
Figure F15. SONNE95 multichannel seismic line used to initially locate Site 1148 (proposed site SCS-5C) at SONNE95, Line 5 (CDP 7500). TWT = two-way traveltime.

Line SO95-5, CDP 7500 (1:57)
Water depth: 3294 m
Penetration depth: 853 mbsf
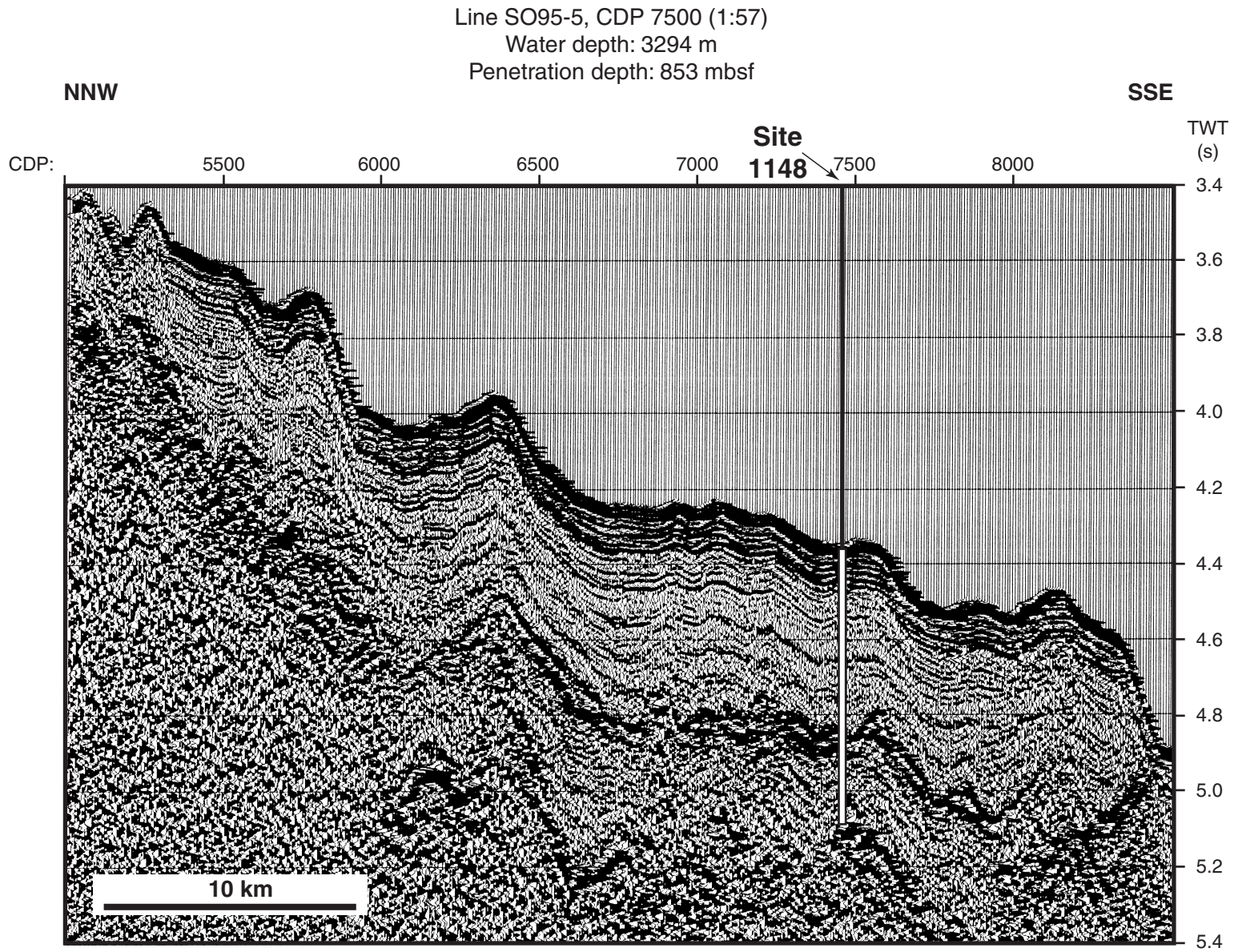
Figure F16. A. *JOIDES Resolution* Leg 184 single-channel seismic line used to define the final location of Site 1148 at *JOIDES Resolution* Leg 184, Line 1 (SP 730). TWT = two-way traveltime. (Continued on next page.)
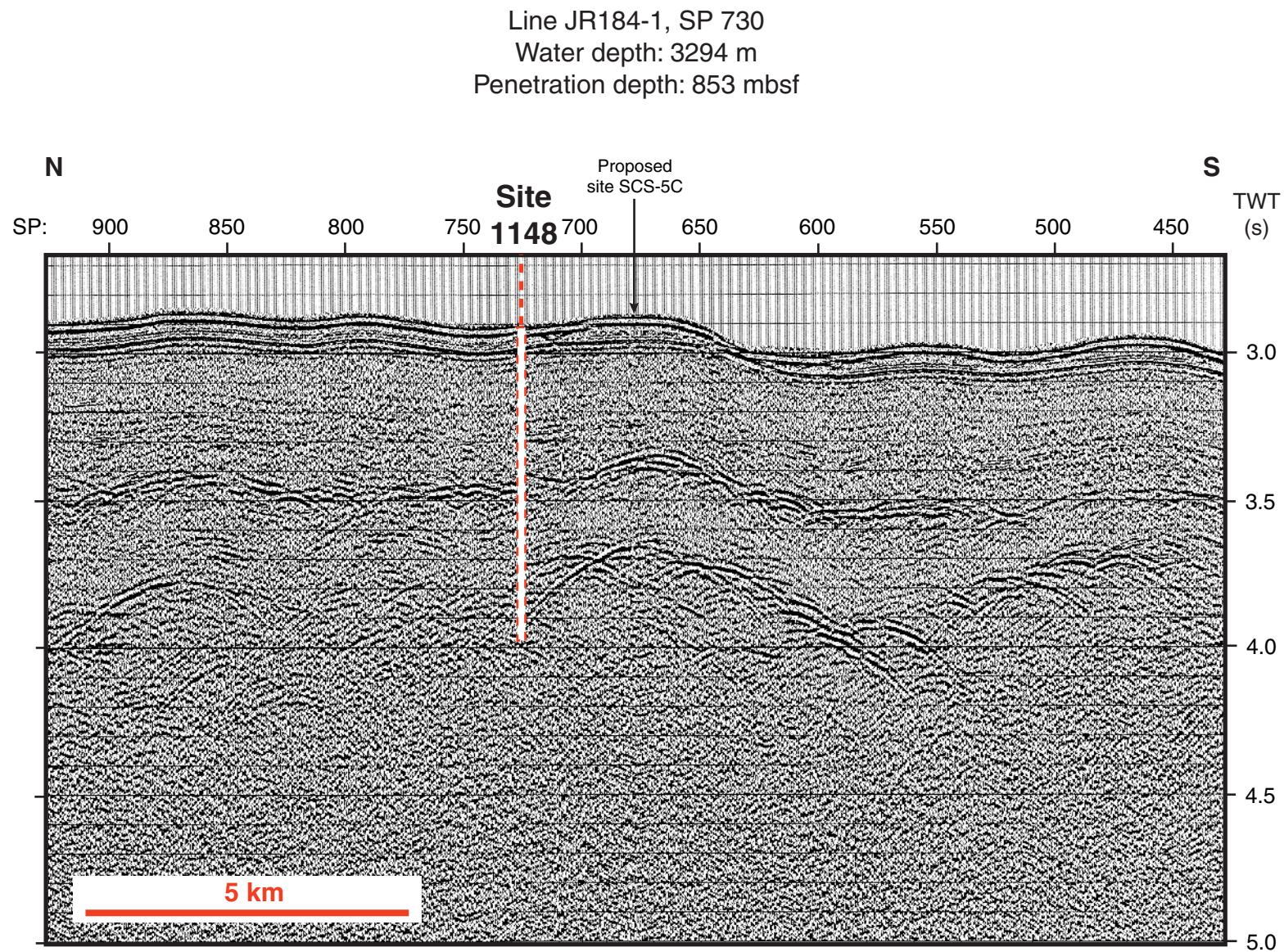
Figure F16 (continued). B. *JOIDES Resolution* Leg 184 single-channel seismic lines used to define the final locations of Sites 1147 and 1148 at *JOIDES Resolution* Leg 184, Line 1 (SP 1940 and 1980, respectively).
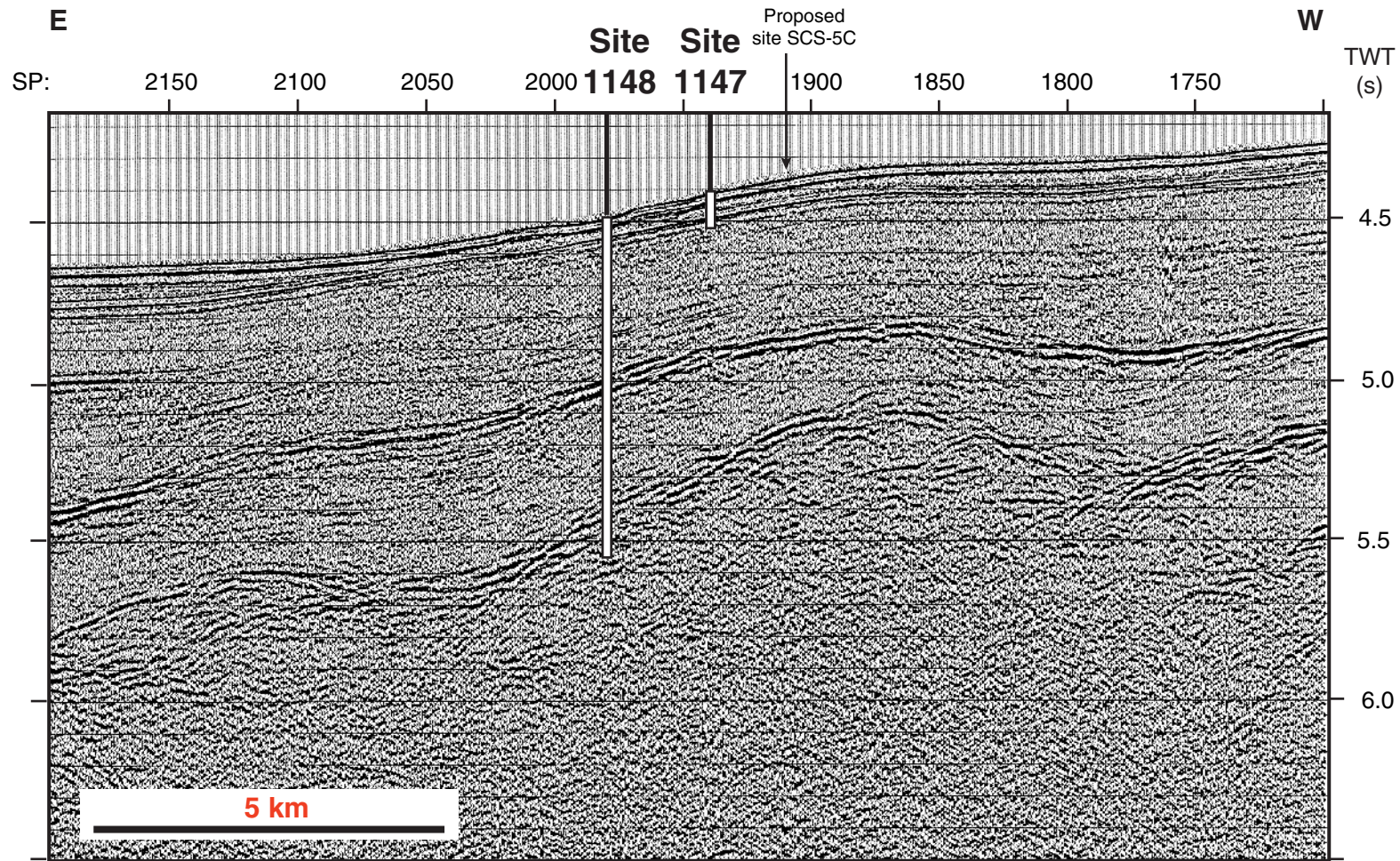
Figure F17. The *JOIDES Resolution* Leg 184 3.5-kHz records across proposed site SCS-5C, near Sites 1147 and 1148. **A.** *JOIDES Resolution* Leg 184, Line 1 (JD71, 0500–0600 hr). JD = Julian day. (Continued on next page.)
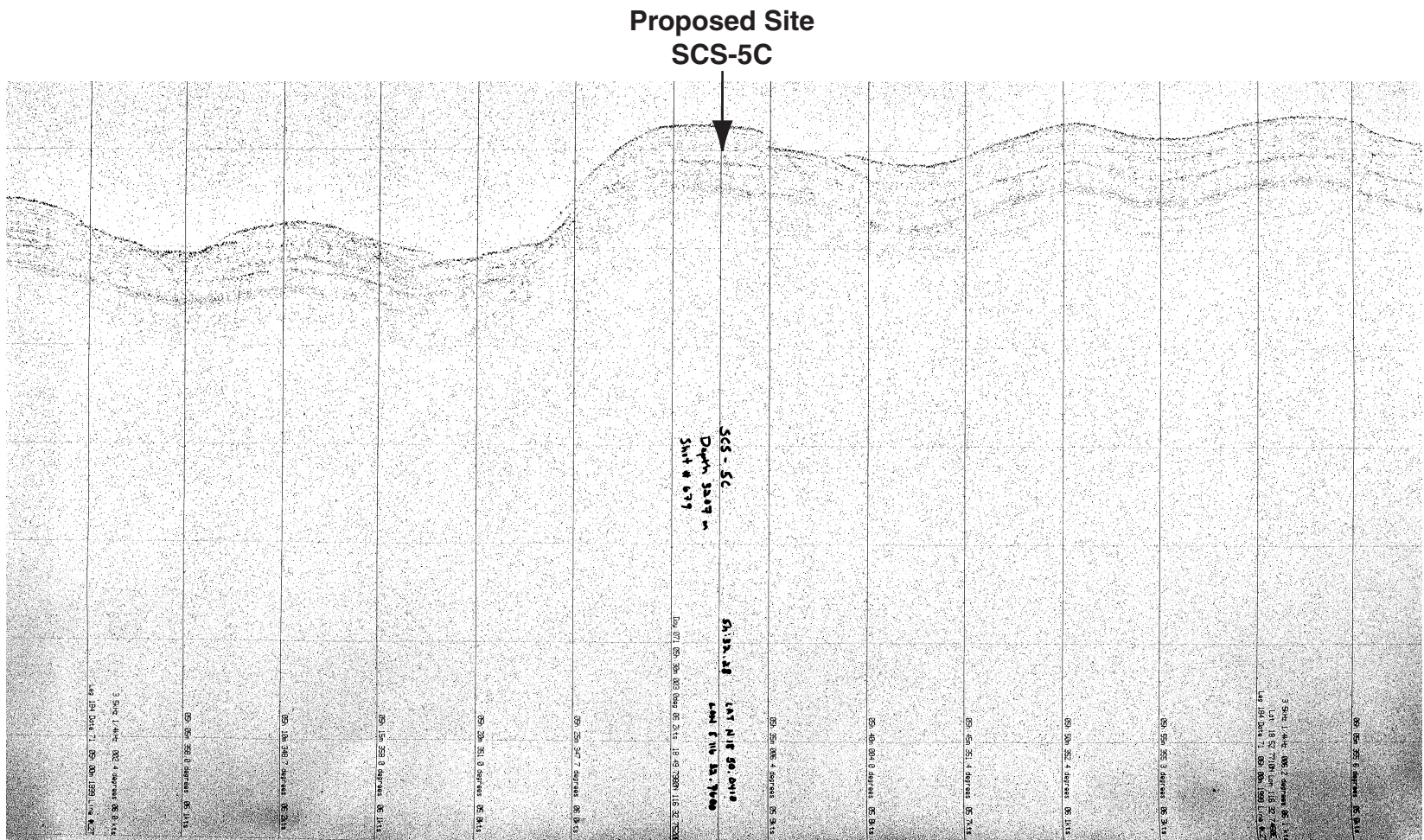
Figure F17 (continued). B. *JOIDES Resolution* Leg 184, Line 1 (JD71, 0840–0940 hr).
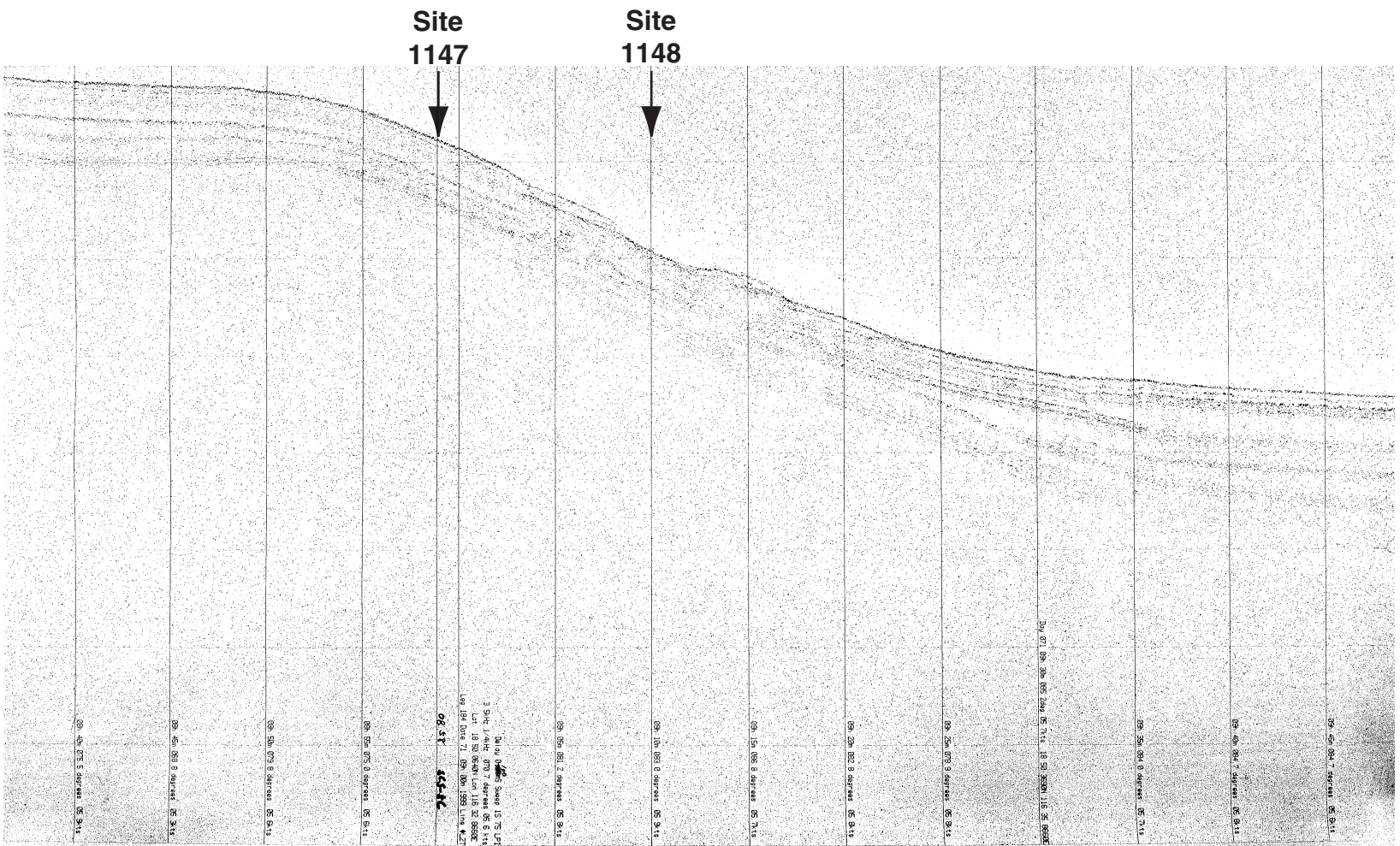
Figure F18. Comparison of the acoustical impedance record with seismic reflector stratigraphy (*JOIDES Resolution* Leg 184, Line 1) at Site 1148. TWT = two-way traveltime.
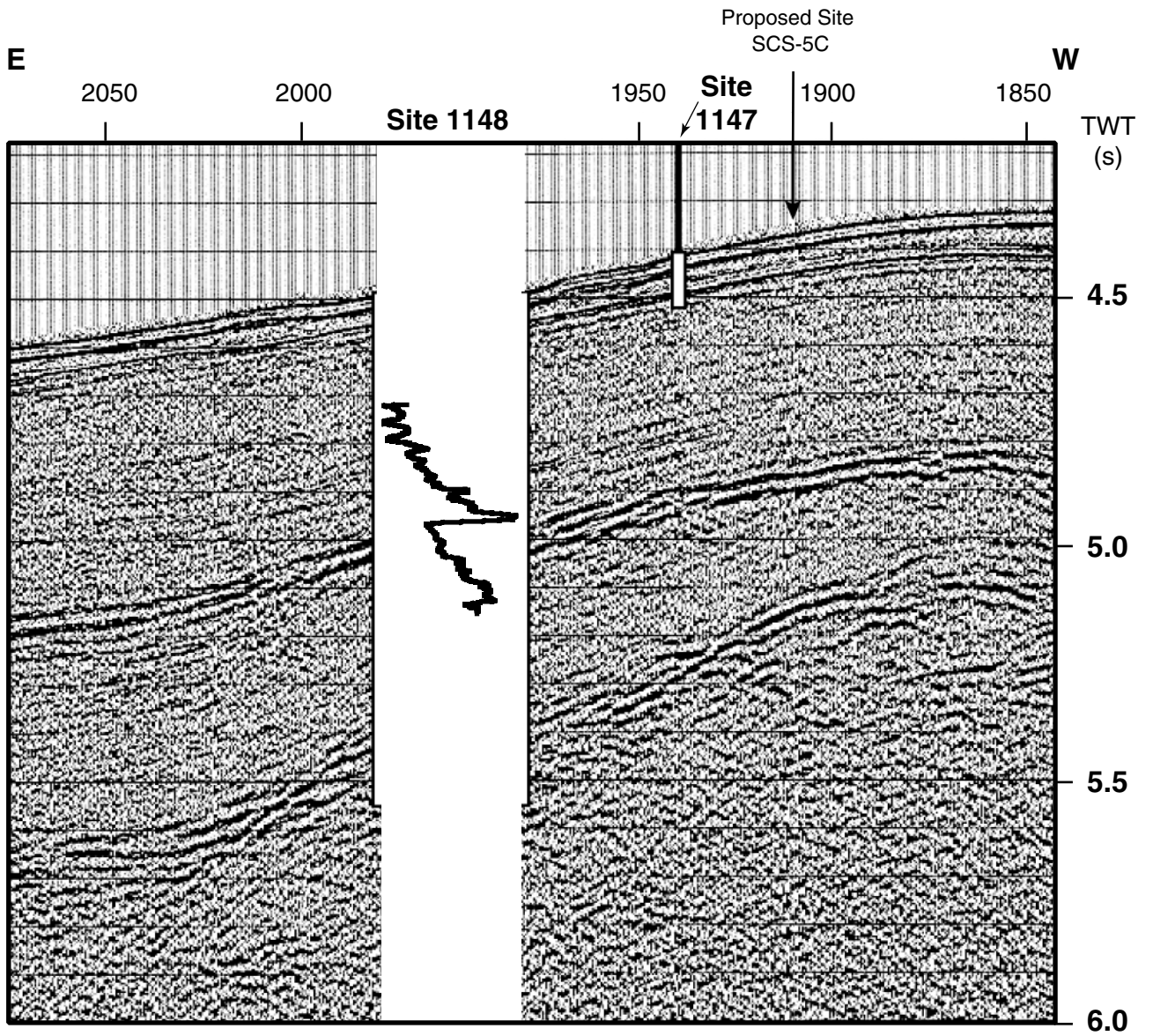
Table T1. Primary seismic lines used to evaluate Leg 184 sites.

Seismic line	CDP/SP	CDP/SP
Site 1143 (SCS-9)		
NSL Line 160	1,681	1,921
NS Line 240	3,521	3,761
Site 1144 (SCS-1)		
SONNE95, Line 10	8,000	11,500
SONNE95, Line 20	1,600	5,250
Site 1145 (SCS-2)		
SONNE95, Line 10	2,800	6,500
Site 1146 (SCS-4)		
SONNE95, Line 5	1	3,700
JR184-1145, Line 3	2,050	2,550
JR184-1145, Line 3	2,950	3,450
Site 1148 (SCS-5C)		
JR184-1148, Line 1	423	925
JR184-1148, Line 1	1,700	2,200
SONNE95, Line 5	5,000	8,500

Notes: Both precruise and *JOIDES Resolution* data are listed. CDP = common depth point, SP = shotpoint, SCS = South China Sea, JR = *JOIDES Resolution,* NS = Nansha, NSL = connecting lines of Nansha.

Table T2. Summary of reflector sequence and age from the Pearl River Mouth Basin (Ludmann and Wong, 1999 [L&W]) and the observed sequence of reflectors at the Leg 184 sites.

Reflector sequence	Epoch	Age (Ma)	Site 1143			Site 1144			Site 1145			Site 1146			Site 1148		
			TWT (s)	Depth (mcd)	Age (Ma)	TWT (s)	Depth (mcd)	Age (Ma)	TWT (s)	Depth (mcd)	Age (Ma)	TWT (s)	Depth (mcd)	Age (Ma)	TWT (s)	Depth (mcd)	Age (Ma)
T_0	Pleistocene	0.45				0.47	370	0.715	0.12	85	0.6						
T_0'	Pliocene/Pleistocene	1.85				0.75	610*	1.23*	0.21	160	1.87	0.2	155	1.36			
T_1	Miocene/Pliocene	5.2	0.27	210	5.2										0.20	175	4.4
T_2	middle/upper Miocene	10.2	0.55	460	9.1							0.5	430	9.8			
T_4	lower/middle Miocene	14	0.67	560*	11.3*												
			0.95	820*	17.0*				1.0	760*	17*						
T_5	Oligocene/Miocene	25.2										0.77	700*	20.9*	0.52	450	22.6
												0.8	740*	22.2*			
T_7	lower Oligocene	32										1.0	950*	29.2*	0.85	790	31.5
															0.90	840	31.8

Notes: TWT = two-way traveltime in seconds. Reflector T_5 is adopted from Chen et al. (1987), as given in table 1 of L&W. We indicate the approximate correlation of Leg 184 reflectors with the L&W sequence. However, in a number of sites (especially Sites 1146 and 1148), we find multiple reflectors over an age interval that roughly correlates with the L&W reflector chronology. * indicates that the estimates of depth and age are derived from downward continuation of the velocity and linear sedimentation rate structure from the base of the cored section. Hence, these estimated values are approximate at best.